



Silicon 3D & SiPM

Maurizio Boscardin

boscardi@fbk.eu

2 Research Centers with a common strategy

- Center for Information Technology
- Center for Materials & Microsystems

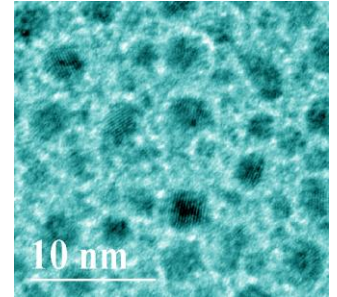
- 118 researchers
- 68 collaborators
- 56 technologists
- 8 secretaries
- 62 PhD students
- 12 visiting professors



MTLab a reliable and a technological updated facility for:

- R&D
- primary-stage product development
- product manufacturing activities

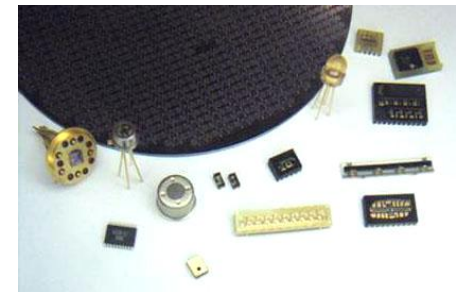
in the area of MEMS, micro and nano technologies.



MicroFabrication Lab

- ✓ Clean Room class 10-100 (500m²) , 1000
increase the clean area dedicated to MEMS process
- ✓ 4" wafers (Si, Quartz, Glass)

Staff: 7 researchers & 9 technicians



DOPING

Ion Implanter (As , B and BF_2 , P) Solid source doping (B and P)

FURNACES for oxidation (wet and dry) and diffusion

LPCVD Silicon oxide (TEOS and LTO), Poly-silicon and Silicon Nitride

PECVD Silicon oxide, Silicon Nitride, Amorphous Silicon

METALLIZATION

Sputtering ($\text{Al}1\%\text{Si}$, Ti, TiN) or Evaporator (Cr, Au, ITO, Ag, ...) or Electrodeposition (Au, ..)

LITHOGRAPHIC EQUIPMENT

Two Mask aligner and two track system and

Stepper (being purchase)

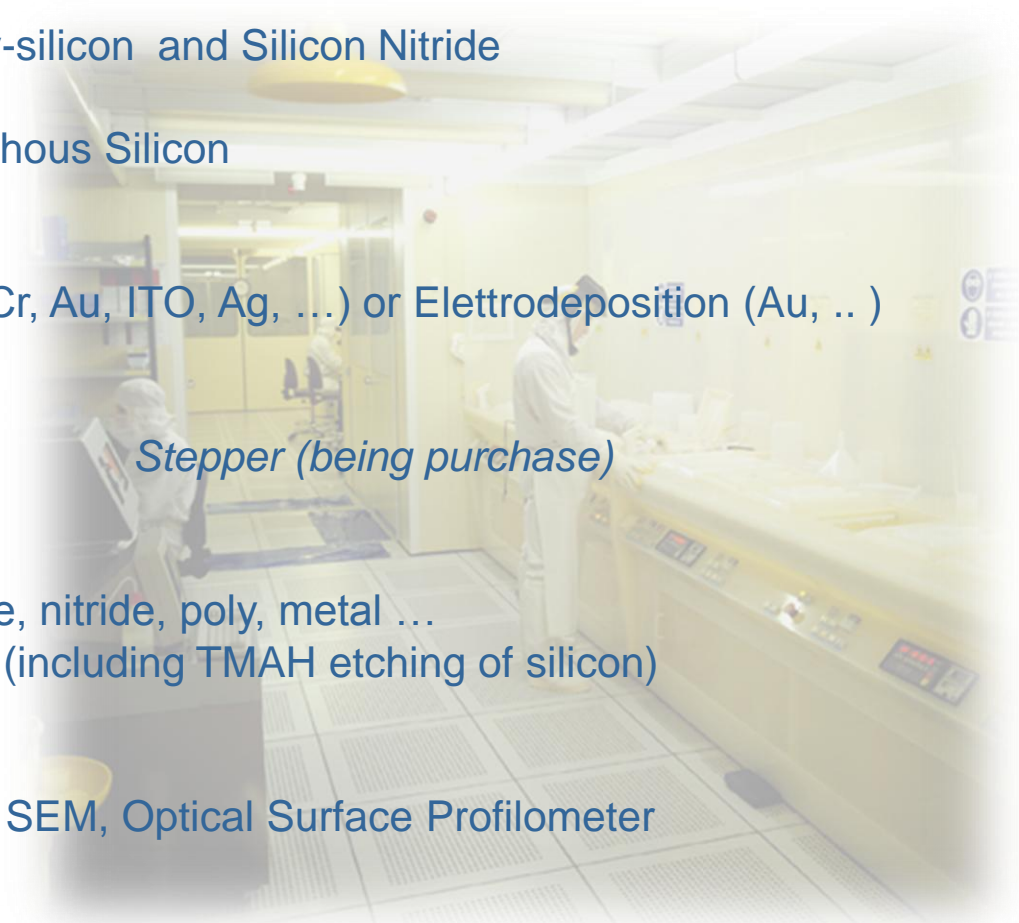
ETCHING

Tegal systems for dry etching of silicon oxide, nitride, poly, metal ...

Deep RIE of silicon and oxide , Wet etching (including TMAH etching of silicon)

ON-LINE INSPECTION

Ellipsometer, Interferometer, 4-point probe, SEM, Optical Surface Profilometer



“Standard” technology

From the specifications given by the customer we design, produce, and (electrical) test the detector.

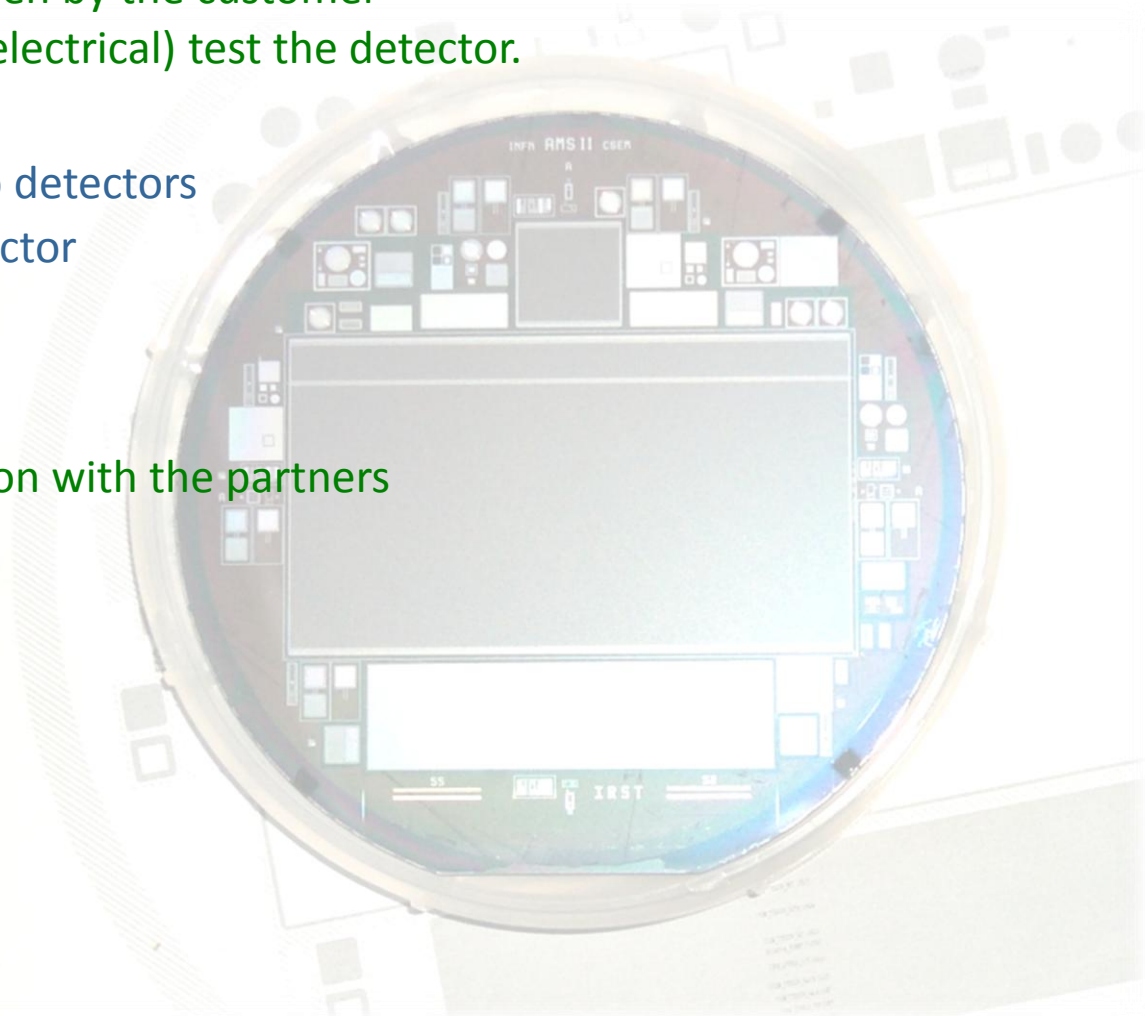
Examples:

- single/double-sided strip detectors
- p-on-n/n-on-n pixel detector

R&D activities

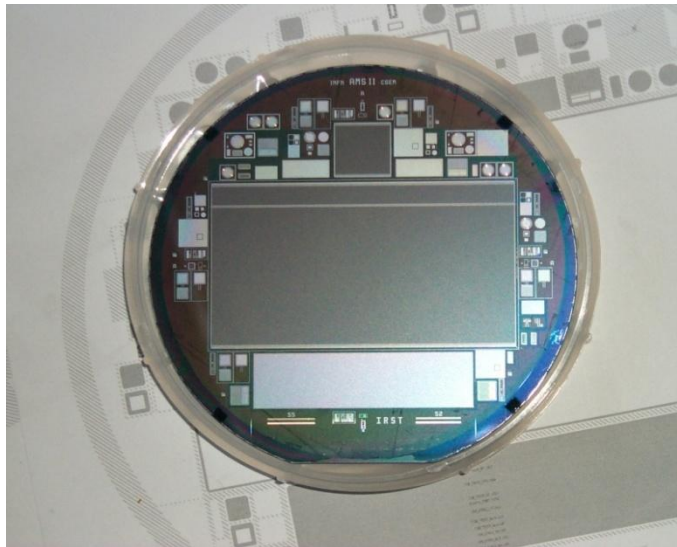
Development in cooperation with the partners

- 3D detectors
- silicon photomultipliers



Standard tech.: strip detectors

AMS experiment (@ISS)

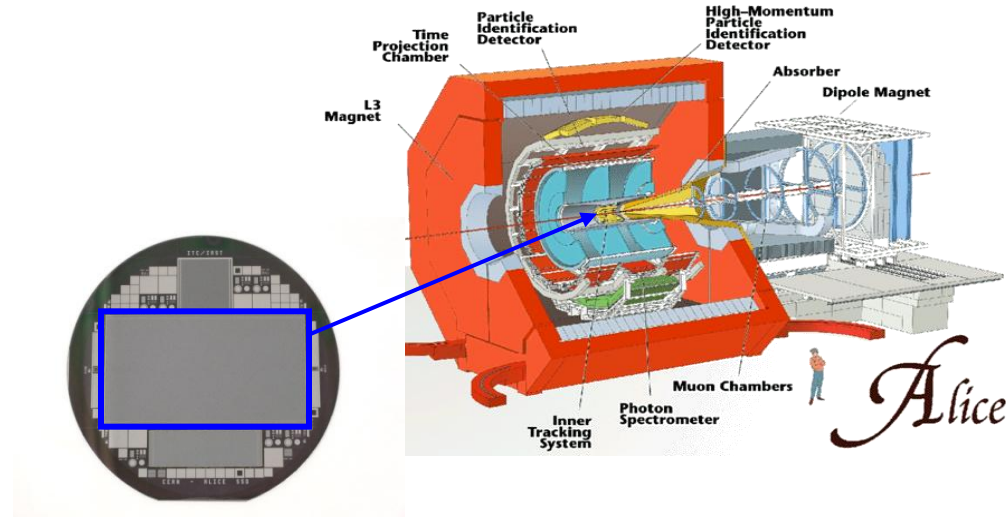


Detector characteristics:

- Area: 7.2x4.2cm²
- double-sided with orthogonal strips
- DC coupled
- spec: defective strips < 0.5% per side

700 in spec detectors were fabricated (2002-2004).

ALICE experiment (@CERN)



Detector characteristics:

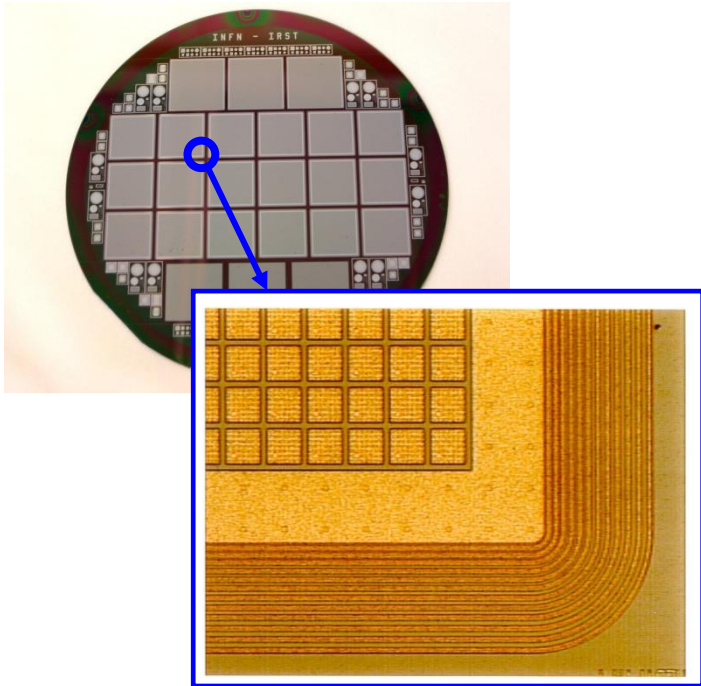
- Area: 7.5x4.2cm²
- double-sided with strips slightly tilted
- AC coupled
- spec: defective strips < 3% per detector

600 in spec detectors were fabricated (2003-2005).

Standard tech.: pixel detectors

Medipix 1&2

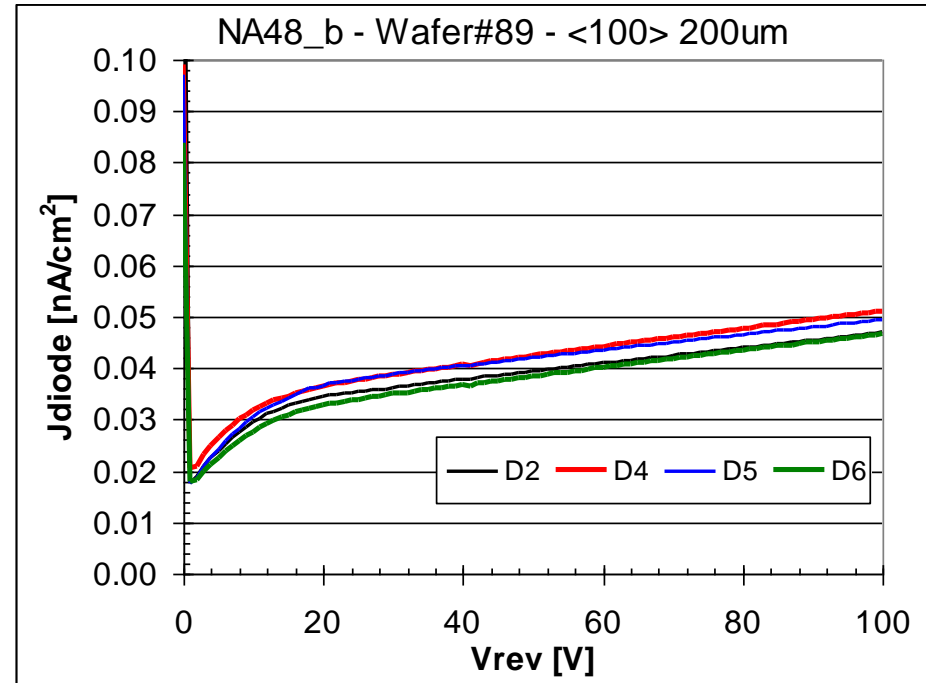
ALICE



Multiguard termination structure

- Medipix1: pixel size 170x170mm²
- Medipix2: pixel size 55x55mm²
- QUAD

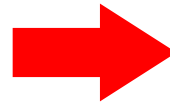
Substrate thick.: up to 1.5mm



Gettering technique to control leakage

- ALICE SPD layout, pixel size 50x400mm²
- NA62 CERN collaboration

Substrate thickness: 200μm



R&D activities

- silicon photomultipliers
- 3D detectors

Ringrazio

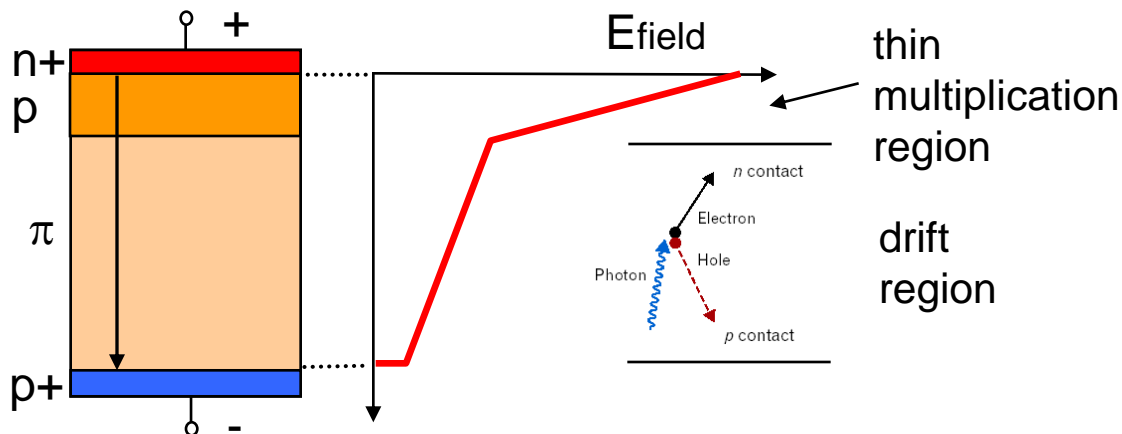
Dr. Claudio Piemonte FBK per le slide sui SiPM

Prof. Gian-Franco dalla Betta Univ. TN per le slide sui 3D

SiPM

Silicon photo multiplier

Realistic structure for an APD

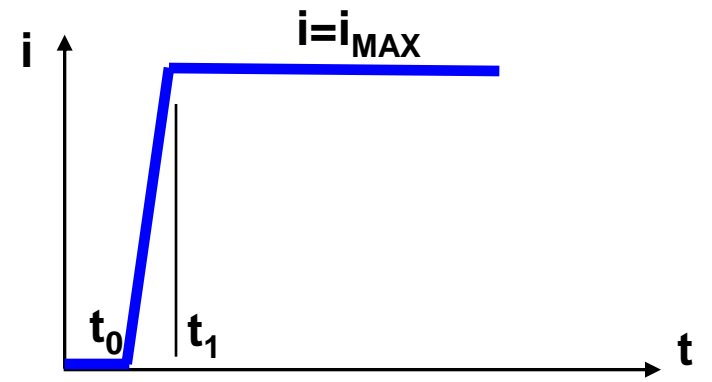


All the electrons photo-generated in the drift region are multiplied (on average) by the same factor!

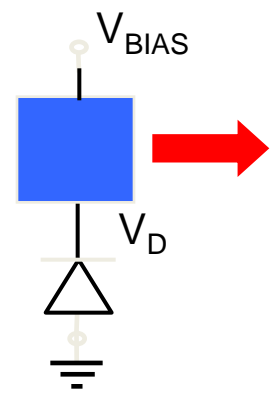
- $V < V_{APD}$
=> **photodiode** 1 collected pair/generated pair
- $V_{APD} < V < V_{BD}$
=> **APD** $\langle M \rangle$ collected pairs/generated pair
- $V > V_{BD}$
=> **Geiger-mode APD** in principle inf. collected pairs/generated pair
SINGLE PHOTON DETECTOR!

Geiger-mode APD

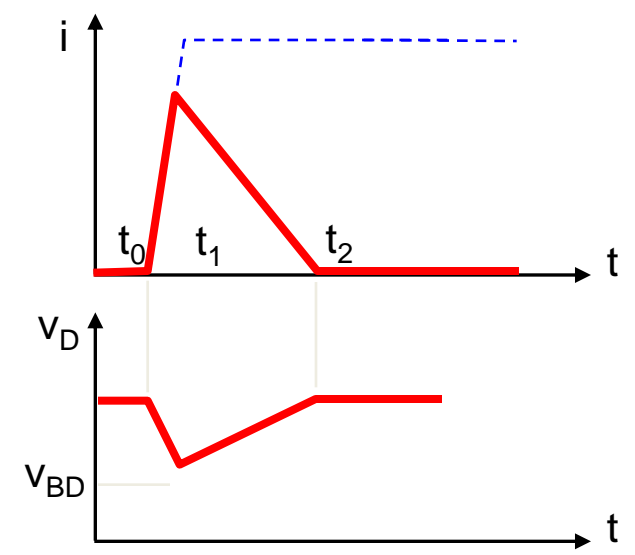
- $t = 0$ let's bias the diode at $V > V_{BD}$
- $t < t_0$ $i=0$ (if no free carriers in the high field region)
- $t = t_0$ photocarrier initiates the avalanche
- $t_0 < t < t_1$ avalanche spreading
- $t > t_1$ self-sustaining current (limited by series resistances)

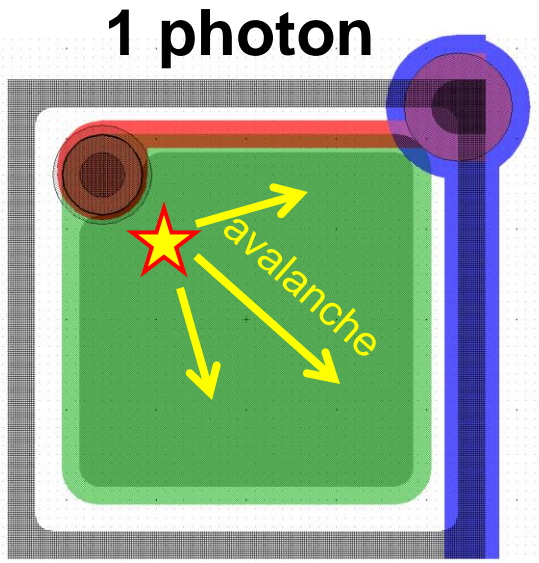


To detect another photon a quenching mechanism is needed!

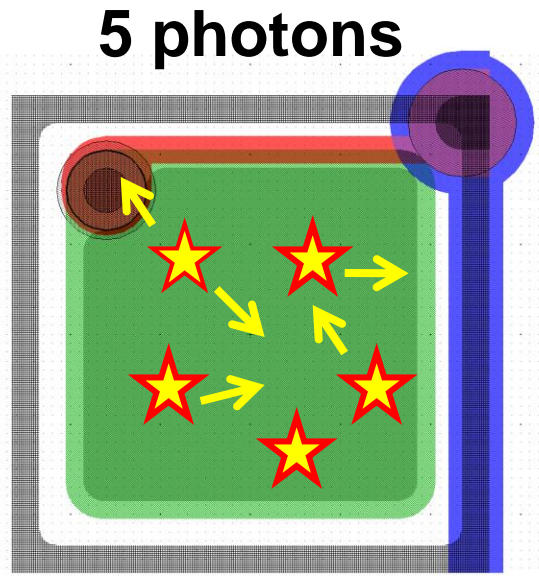


- Two solutions:**
- large resistance: **passive quenching**
 - analog circuit: **active quenching**

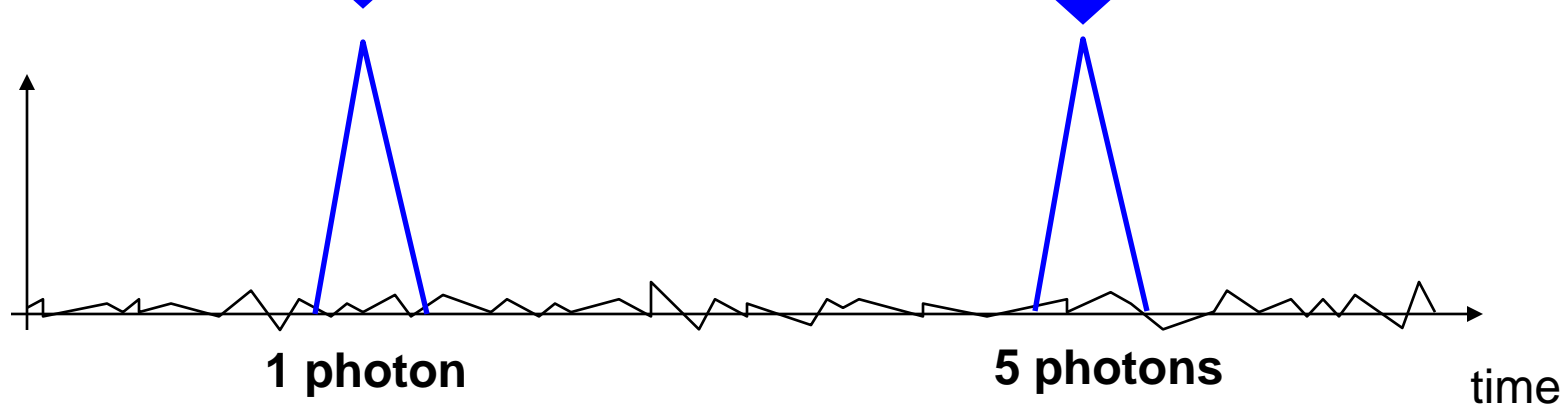




avalanche propagates all over the diode



Current

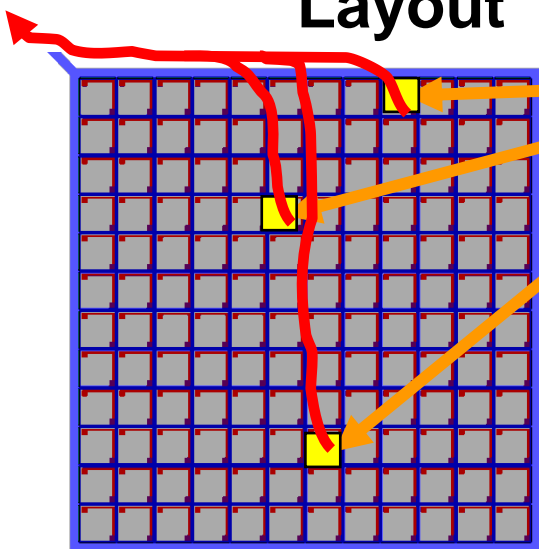


With GM-APDs you cannot count the number of photons

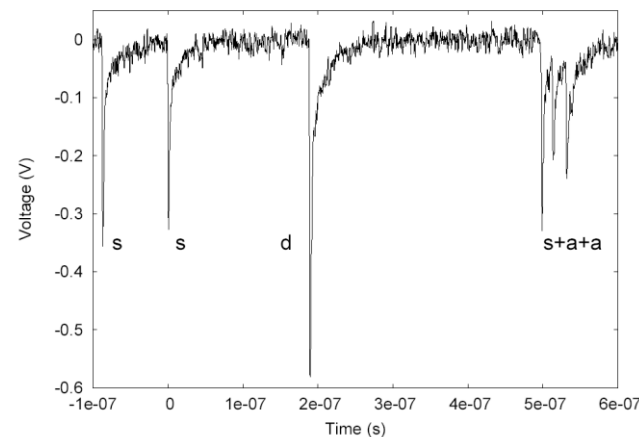
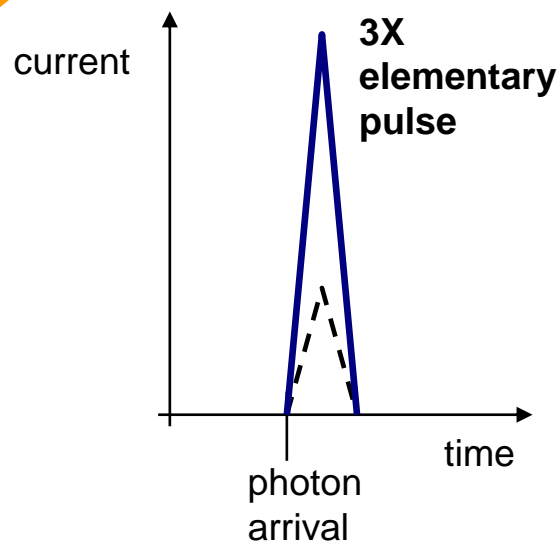
How to count photons? parallel of mini-GM-APDs

first proposed by Golovin and Sadygov in the '90s

Layout



Flash of 3 photons



Proprieties:

- Single photon sensitivity
- Response proportional to number of photons (up to few hundred)
- Extremely good timing resolution (tens of ps)

Features of a SiPM

Most important features of a SiPM are:

- **capability to detect extremely low photon fluxes** giving a proportional information;
- **extremely fast response** (determined by avalanche discharge): in the order of few hundreds of ps.

Other features are:

- Low bias voltage (<100V)
- Low power consumption
- Insensitive to magnetic fields
- Compact and rugged



**extremely interesting
alternative to PMTs**

Problematics (apart from technological):

- temperature dependence of dark count and gain
- low radiation resistance (generation and trapping centers)

Labs developing SiPMs

Pioneering work in the 90's by russian institutes

- JINR, Dubna
 - Obninsk/CPTA, Moscow
 - Mephi/PULSAR, Moscow
- **Metal-Resistive-Semiconductor**
→ polysilicon resistor

Recently, more institutes/companies involved in SiPM production:

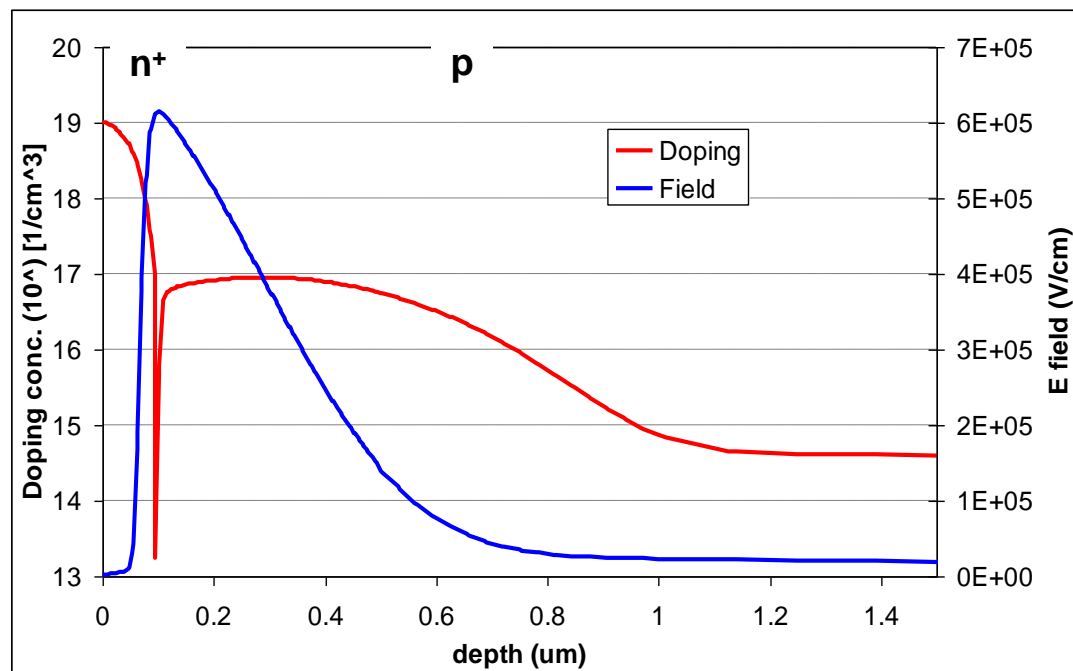
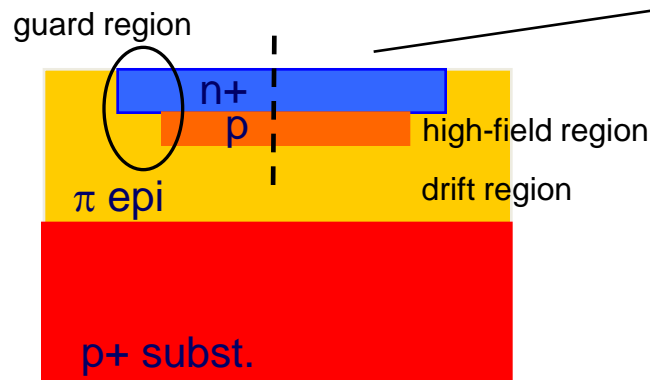
- Hamamatsu, Japan
- SensL, Ireland
- IRST, Italy
- MPI, Germany
- Zecotek, Canada

Front-side illumination
devices available

Back-side illumination;
device ready by end 2007

IRST technology

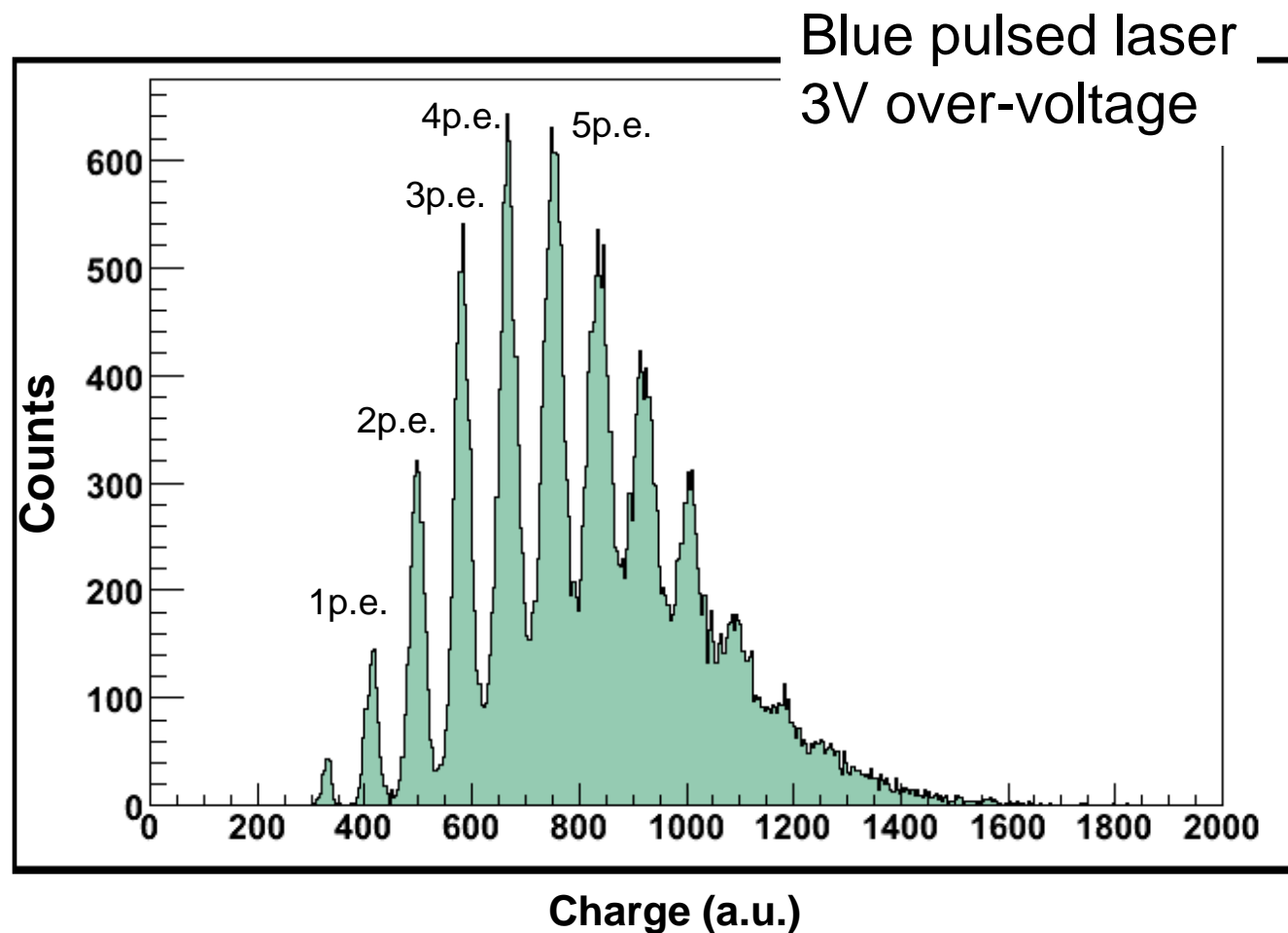
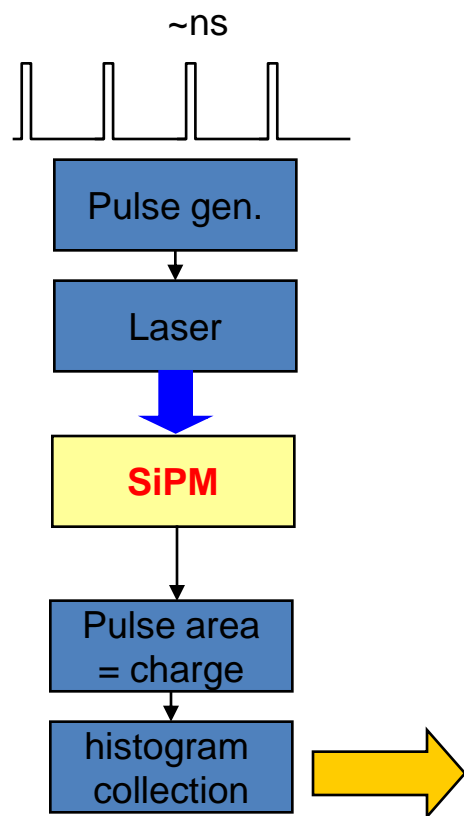
Shallow-Junction SiPM



High field region ← | → Drift region

- 1) Substrate: p-type epitaxial
- 2) Very thin n+ layer
- 3) Quenching resistance made of doped polysilicon
- 4) Anti-reflective coating optimized for $\lambda \sim 420\text{nm}$

Single-cell charge resolution



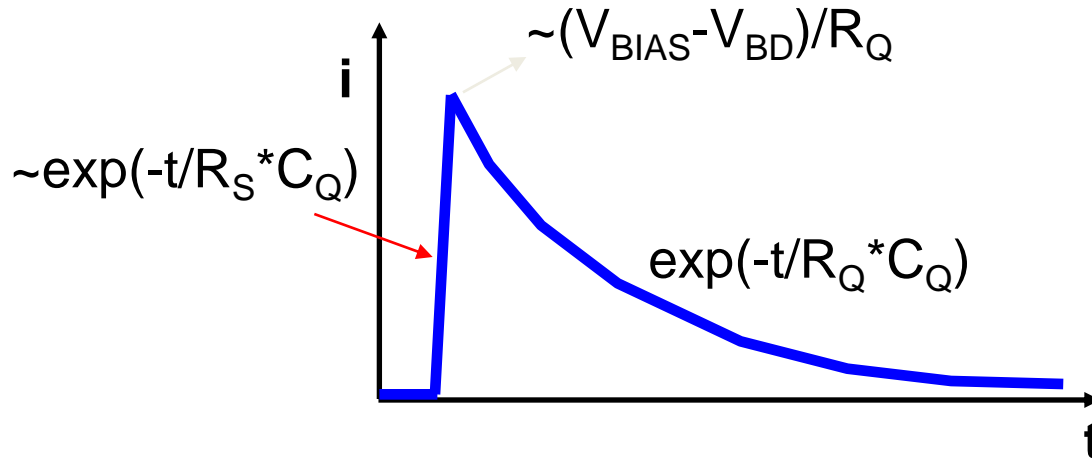
It is possible to count the number of photons in a light pulse

Important parameters in a SiPM

- **Gain** → Number of electrons per photon detected
- **Noise**: primary dark count; secondary: after-pulse; optical cross-talk; → pulses triggered by non-photogenerated carriers
- **Photodetection efficiency** →
$$\frac{\text{Number of counts over}}{\text{Number of impinging photons}}$$
- **Dynamic range** → Linearity of the response
- **Time resolution** → Precision in the determination of the photon arrival time

Gain in a GM-APD

Gain = number of electrons per photon absorbed



charge collected per event is the area of the exponential decay which is determined by circuital elements and bias.

$$\text{Gain} = I_{\text{MAX}} \frac{\tau_Q}{q} = \frac{(V_{\text{BIAS}} - V_{\text{BD}}) * \tau_Q}{R_Q q} = \frac{(V_{\text{BIAS}} - V_{\text{BD}}) * C_D}{q}$$

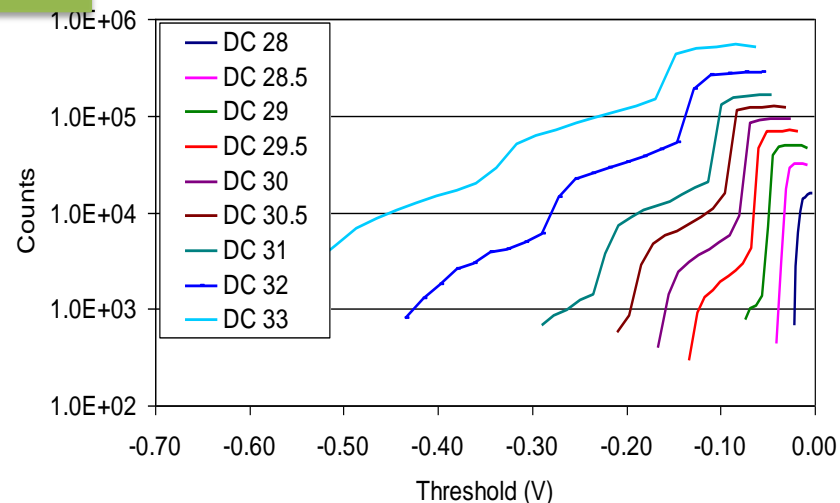
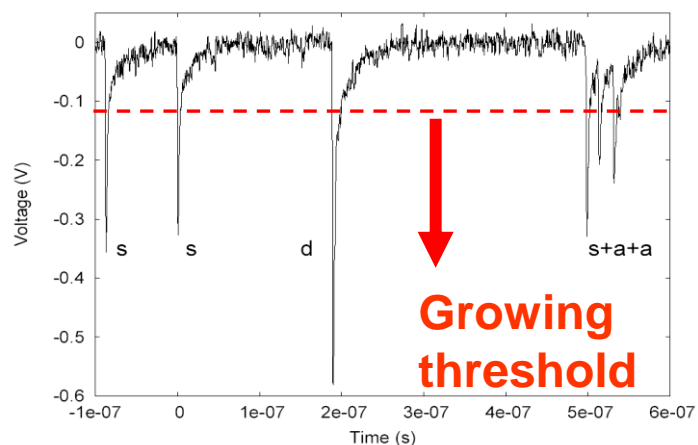
Primary DARK COUNT

False current pulses triggered by non photogenerated carriers

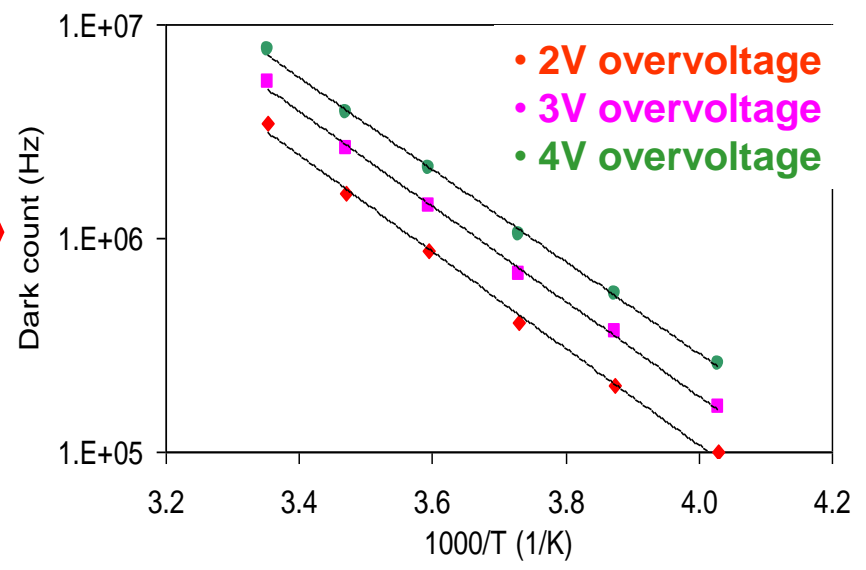
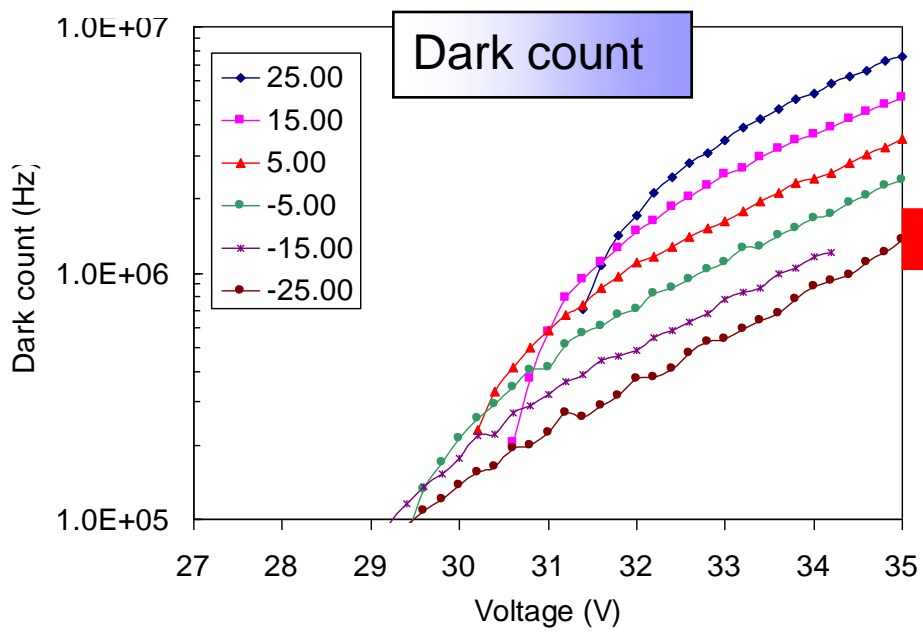
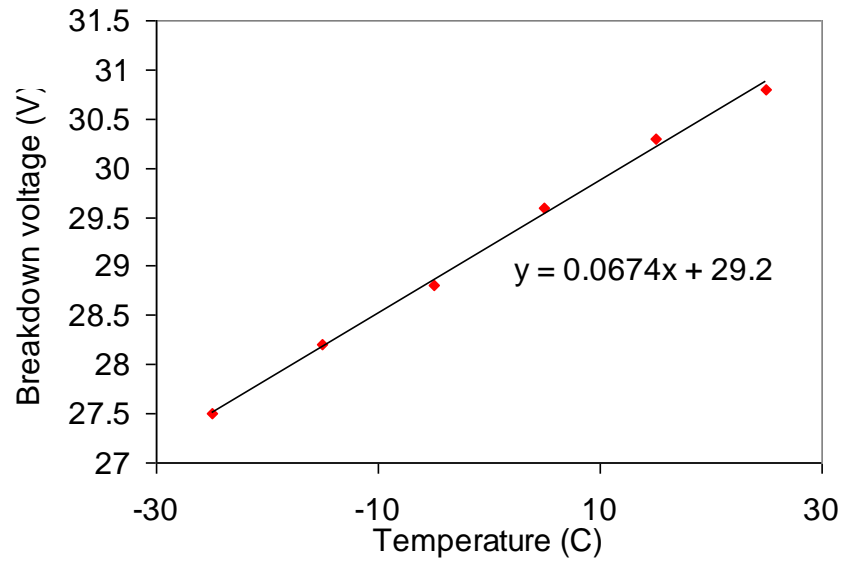
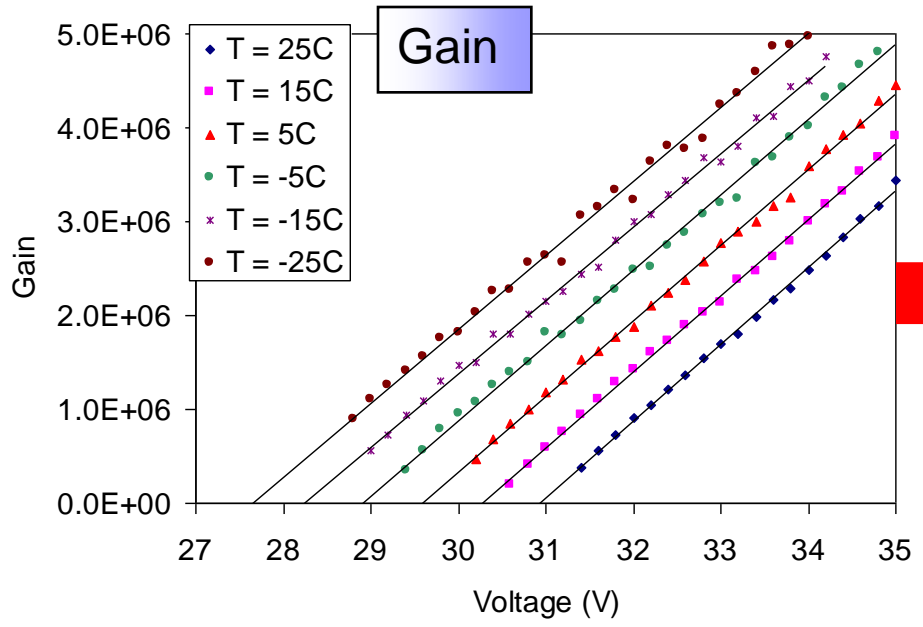
Main source of carriers: **thermal generation in the depleted region.**

Critical points: **quality of epi silicon; gettering techniques.**

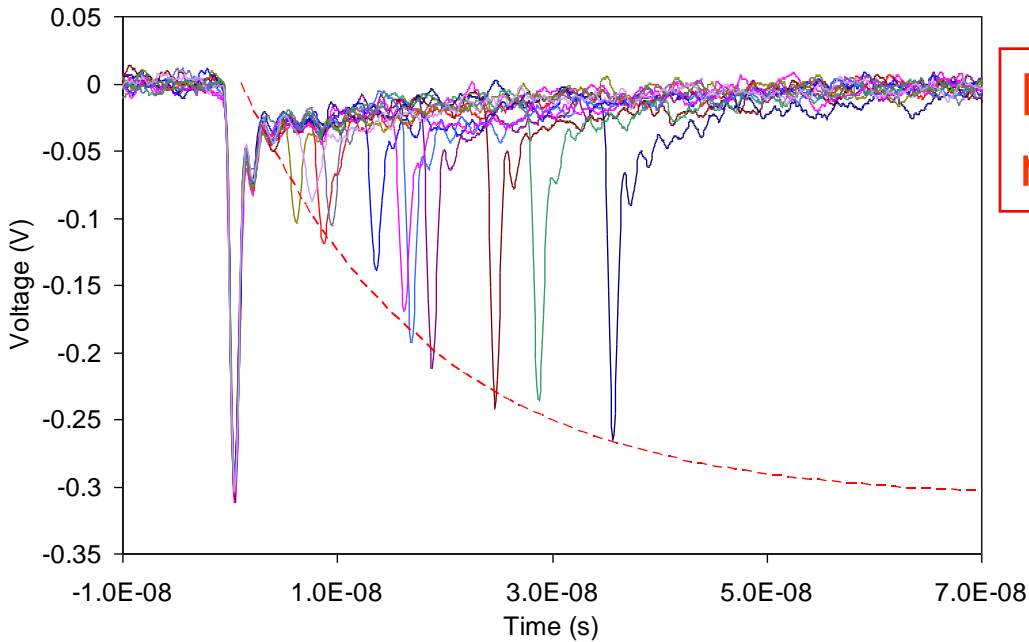
Dark count rate as
a function of the threshold
and the temperature



Temperature dependence



Afterpulse



Events with after-pulse measured on a single micropixel.

The amplitude of the after-pulse increases as the cell recovers to its operational condition

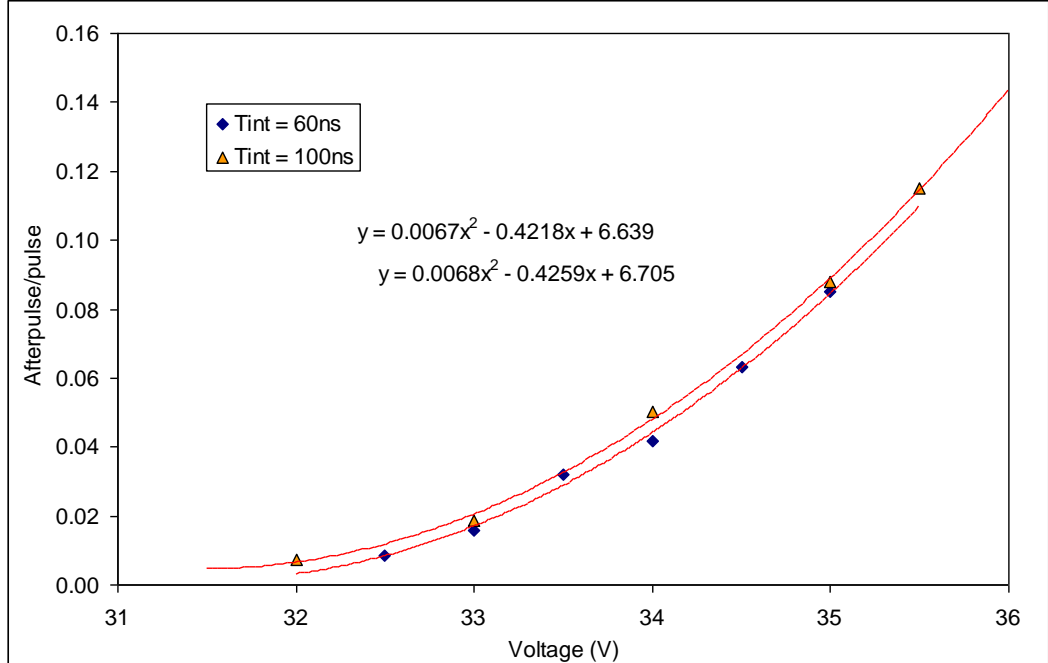
After-pulse probability vs bias

It increases following a parabolic law:

$$P_a = P_c \cdot P_{01}$$

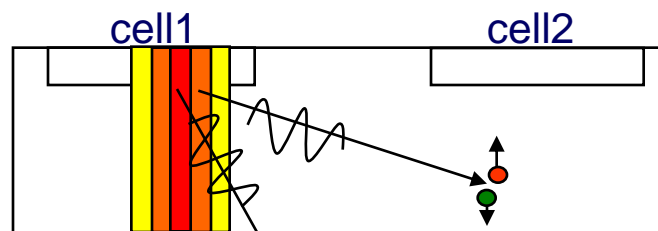
linear with Vbias

linear with Vbias



During an avalanche discharge, photons are emitted mainly because of spontaneous direct carrier relaxation in the conduct. band.

3×10^{-5} photons with energy higher than 1.14eV emitted per carrier crossing the junction. [from A. Lacaita et al., IEEE TED, vol. 40, n. 3, 1993]

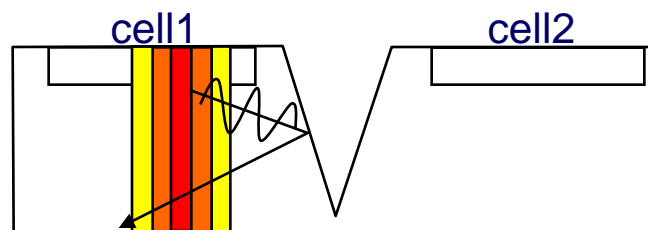


Those photons can trigger the avalanche in an adjacent cell: optical cross-talk.

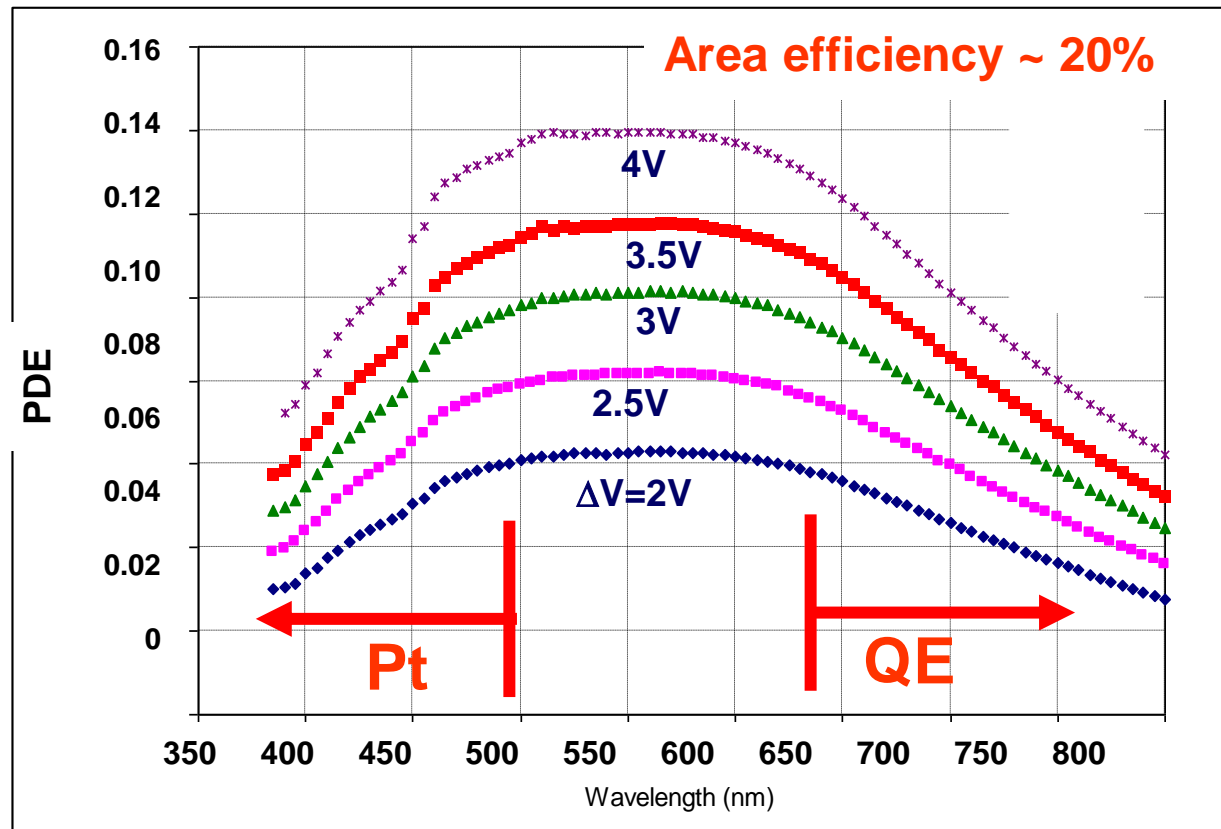
Depends on: - distance between the high-field regions
- gain

Solution:

trenches in silicon filled with opaque material



PDE - result



Why this shape?

$$PDE = QE(\lambda) * Pt(\lambda) * Ae$$

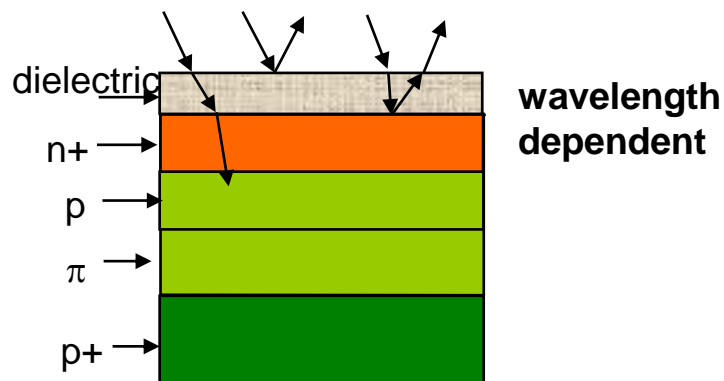
- QE = quantum eff.
- P_t = avalanche prob.
- A_e = area eff.

Photodetection efficiency (1)

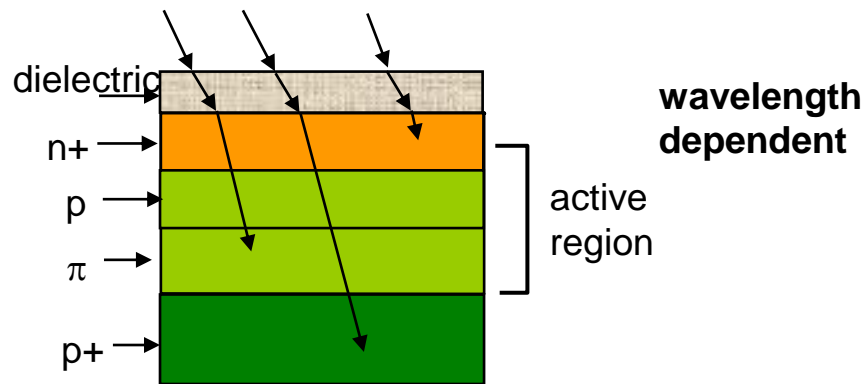
$$\text{PDE} = N_{\text{pulses}} / N_{\text{photons}} = \text{QE} \times P_{01} \times Ae$$

1. **QE** Quantum efficiency is the probability for a photon to generate a carrier that reaches the high-field region.

a. Transmission efficiency



b. Internal quantum efficiency



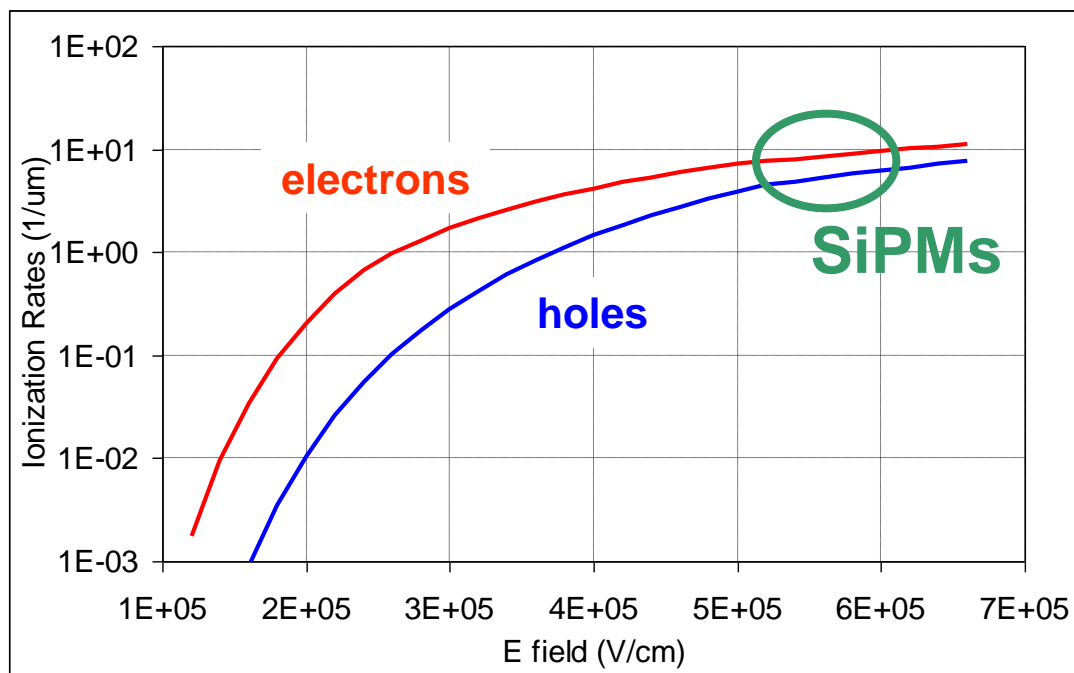
Optimization:

- Anti-reflective coating
- shallow junctions for short λ
- thick depletion layer for long λ

PDE (2)

2. P_{01} . triggering probability

probability for a carrier traversing the high-field to trigger the avalanche.



Ionization rates in Silicon

1. Electrons higher ionization rate. Difference decreases for higher fields, e.g. at $6e5V/cm$ $\alpha_n/\alpha_p \sim 2$.
2. Ioniz. rates increase with field

P_{01} maximization:

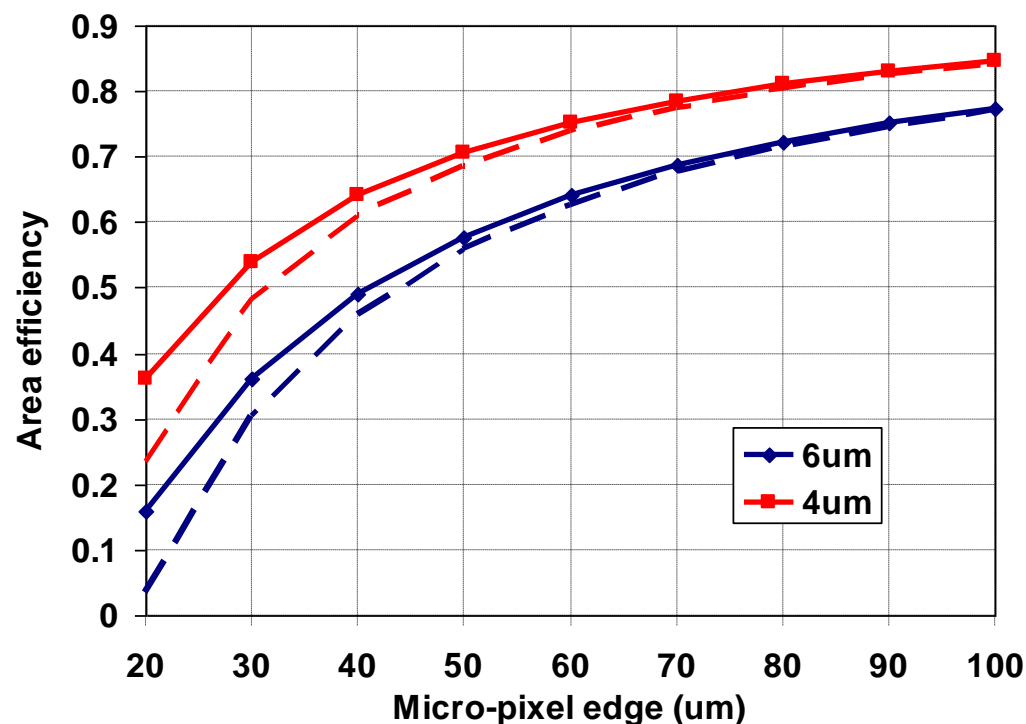
1. high overvoltage

2. photo-generation in the p-side of the junction
(electrons travel through the high-field region)

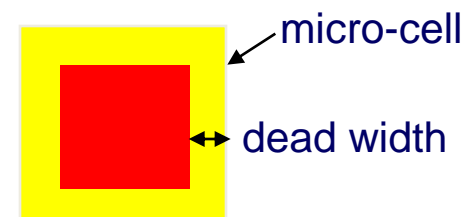
PDE (3)

3. Ae. Area efficiency

"standard" SiPMs suffer from low Ae due to the structures present around each micro-cell (guard ring, trench)



Maximum Ae for a width of the dead region of 4 and 6 μm (in a front-side illuminated SiPM)

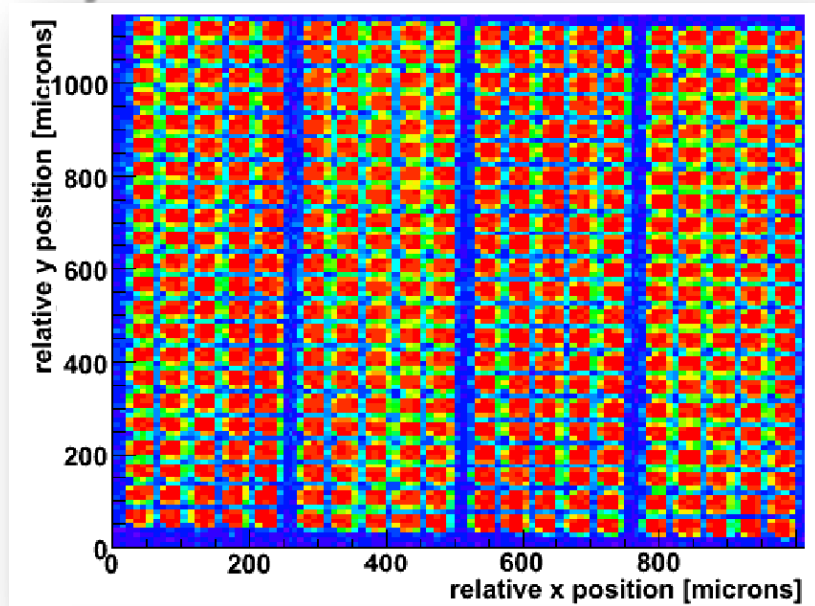


These values can be lower if the polysilicon resistor overlaps the high field region (dashed lines: 50 μm^2 overlap).

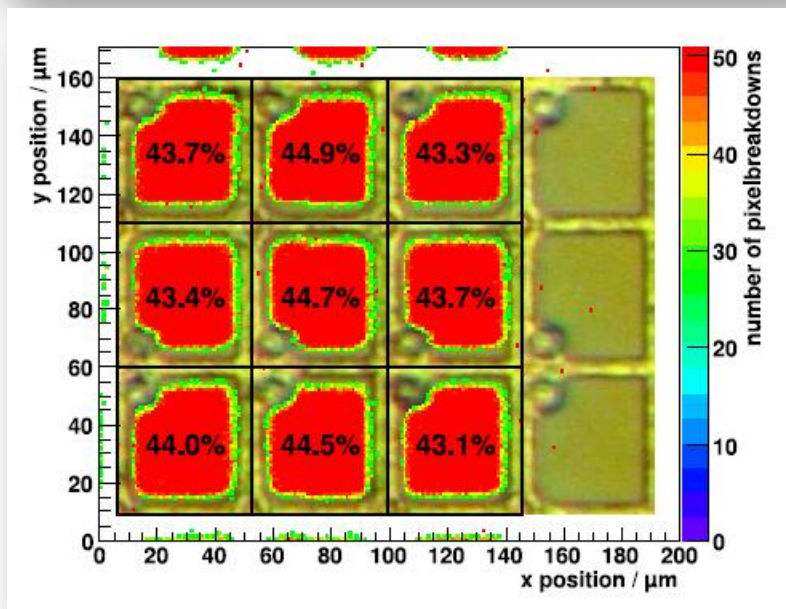
Cell functionality and fill factor

Illumination with a LED.
Spot diameter of $\sim 5 \mu\text{m}$.

Coarse step to verify
functionality of cells

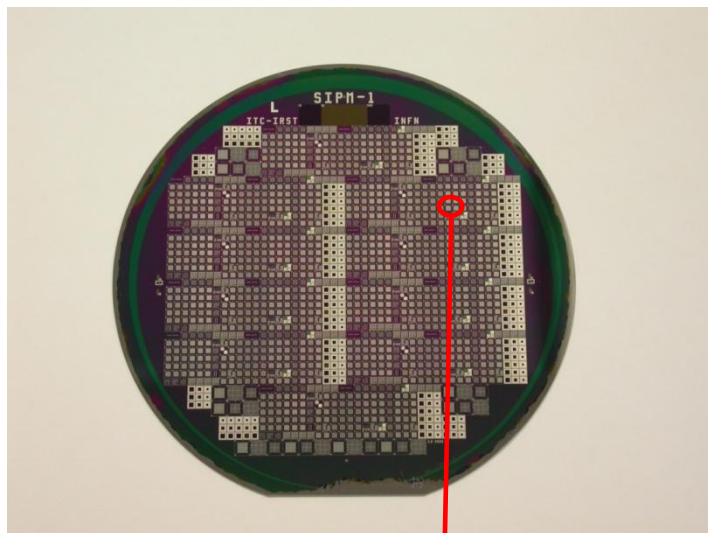


Fine step to estimate the fill
factor



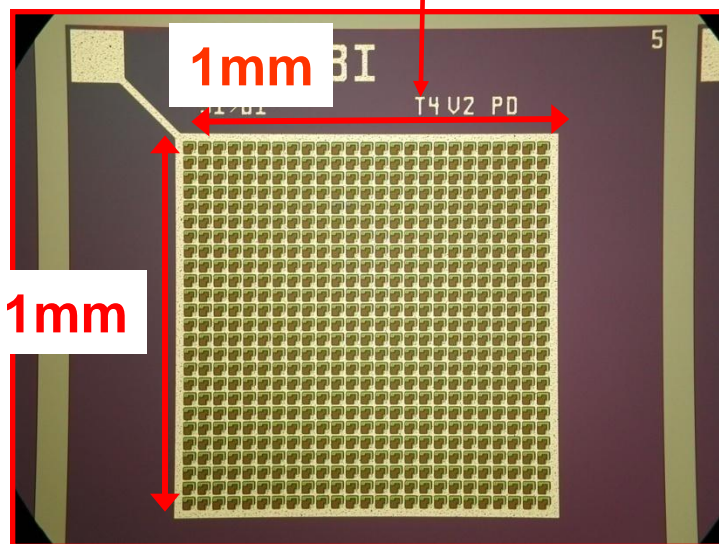
R. Greim, H. Gast, T. Kirn, J. Olzem, G. Roper
Yearwood, S. Schael, N. Zimmermann,
G. Ambrosi; R. Battiston; C. Piemonte
presented at Siena conference 2008

FBK Device geometry: 2005



The wafer layout includes many structures:

- SiPMs;
- GM-APDs;
- "large-area" diodes;
- several test structures

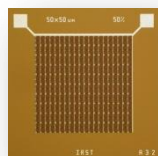


Basic structure:

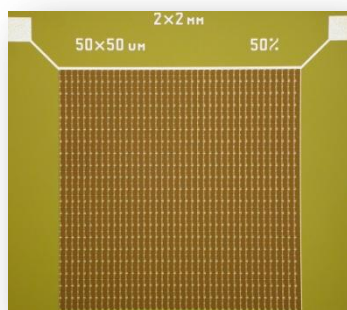
- 25x25 cells
- microcell size: $40 \times 40 \mu\text{m}^2$

Fill factor ~ 30%

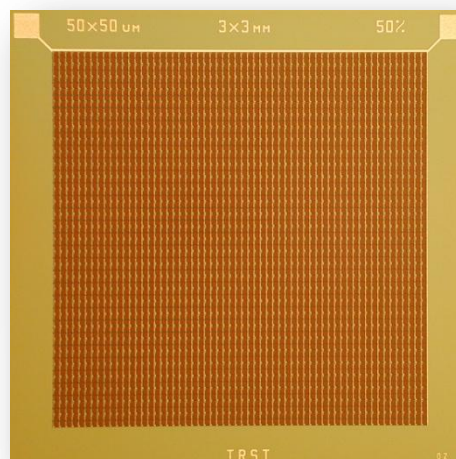
FBK Device geometry 2007



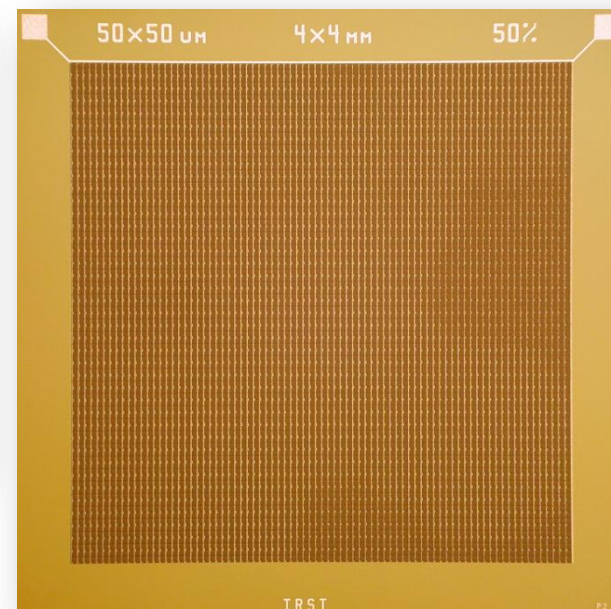
1x1mm²



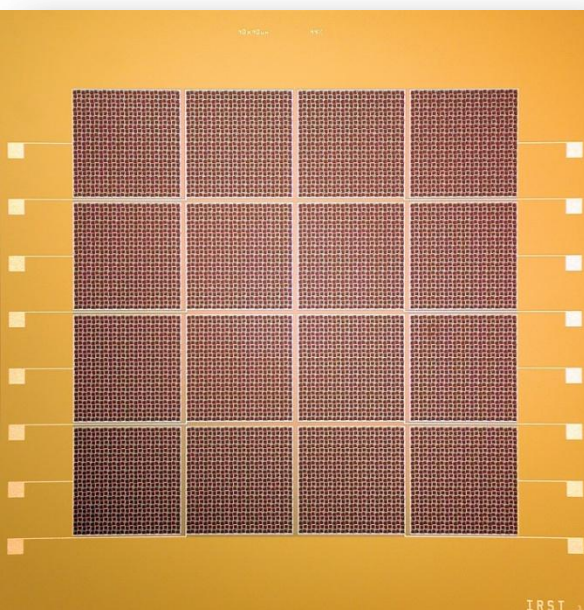
2x2mm²



3x3mm² (3600 cells)

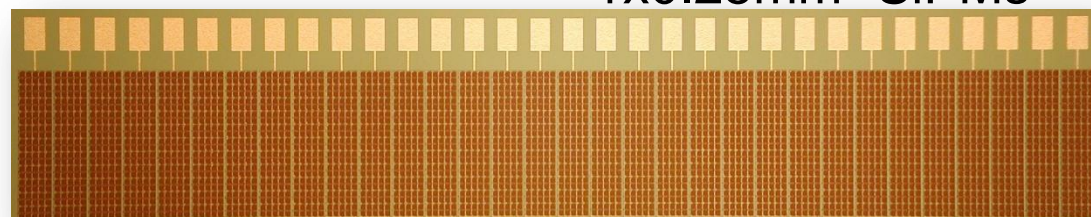


4x4mm² (6400 cells)



Matrices:
4x4 elements
of 1x1mm² SiPMs

Linear arrays:
8,16,32 elements of
1x0.25mm² SiPMs



APPLICAZIONI

High energy physics

- ✓ low light level detection
- ✓ scintillation light readout

astrophysics / “space” experiments

- ✓ Cherenkov and Fluorescence light detection
- ✓ Liquid Xenon detector

medical applications

- ✓ time resolution

EU FP7 PET/MR Project: HYPERImage

www.hybrid-pet-mr.eu

PHILIPS
sense and simplic

MEDISIP

IBBT

UNIVERSITÄT HAMBURG
Universitätsklinikum Hamburg-Eppendorf

FONDAZIONE BRUNO KESSLER

NKI-AVL

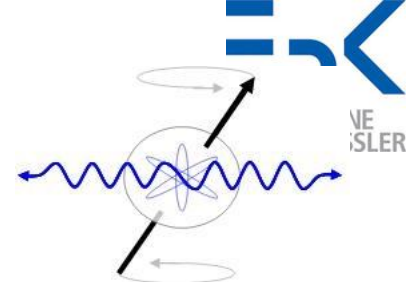
HYPER IMAGE

University of Heidelberg

KING'S College LONDON

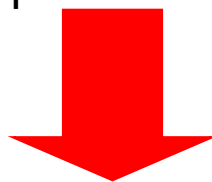
GOBIERNO DE ESPAÑA
MINISTERIO DE CIENCIA E INNOVACION

cnic



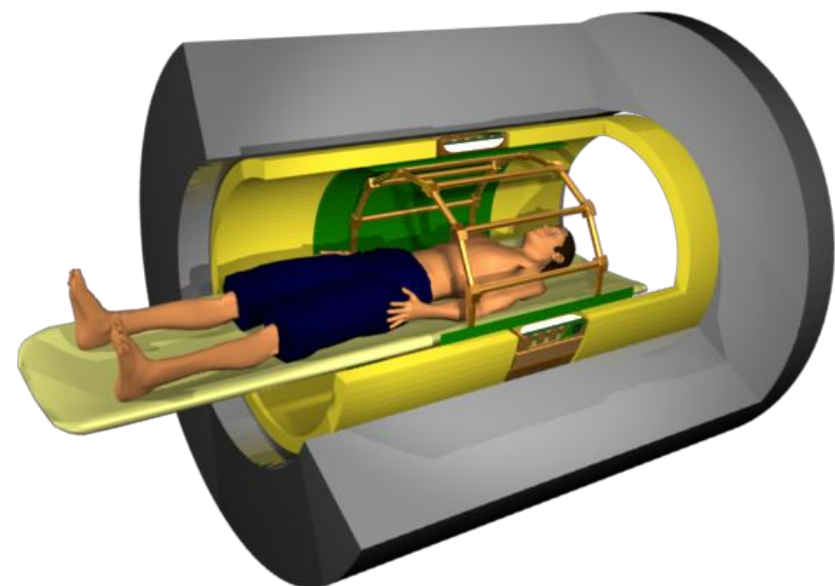
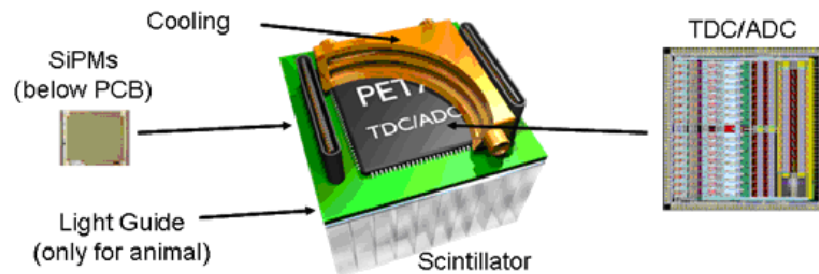
HYPERRimage project

Development of **hybrid TOF-PET/MR** test system with dramatically improved effective sensitivity

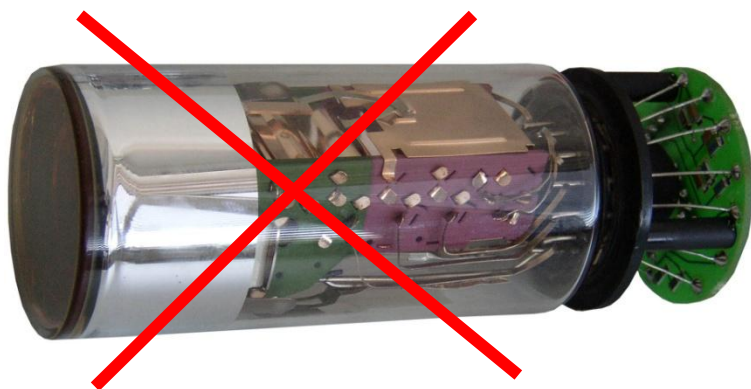


First clinical whole body PET/MR investigations of breast cancer

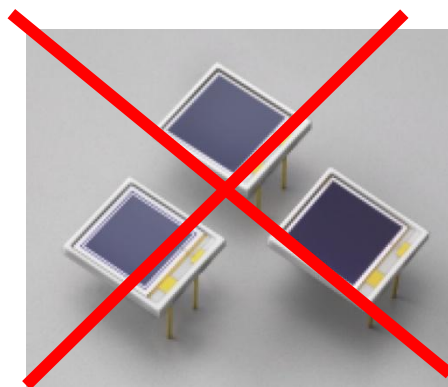
TOF-PET building blocks



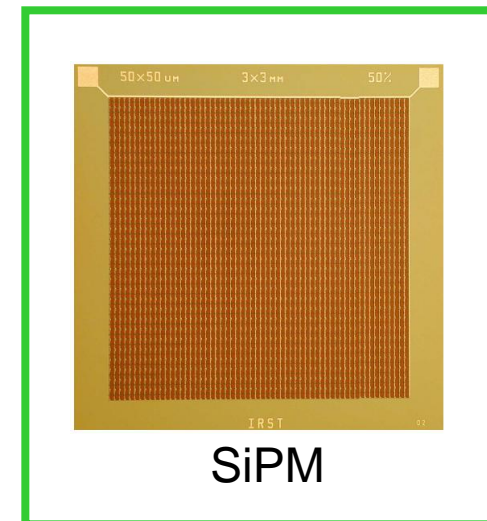
Different Sensor Technologies



PMT



APD

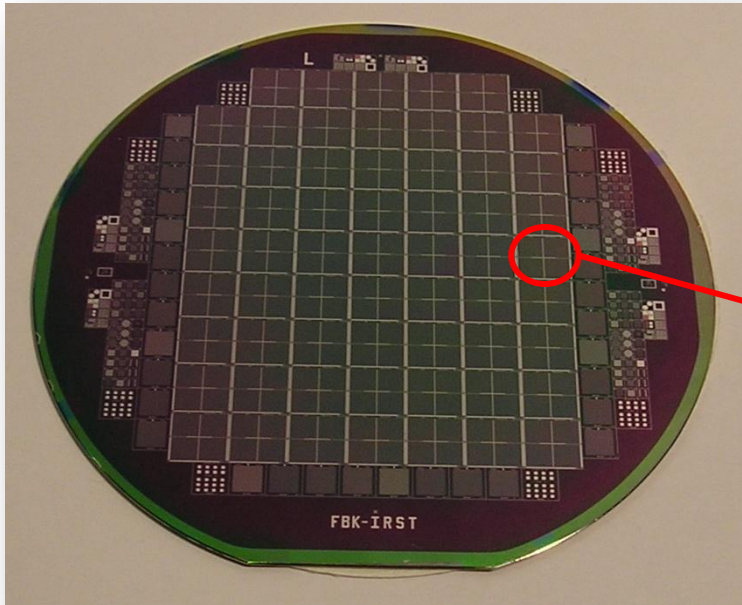


SiPM

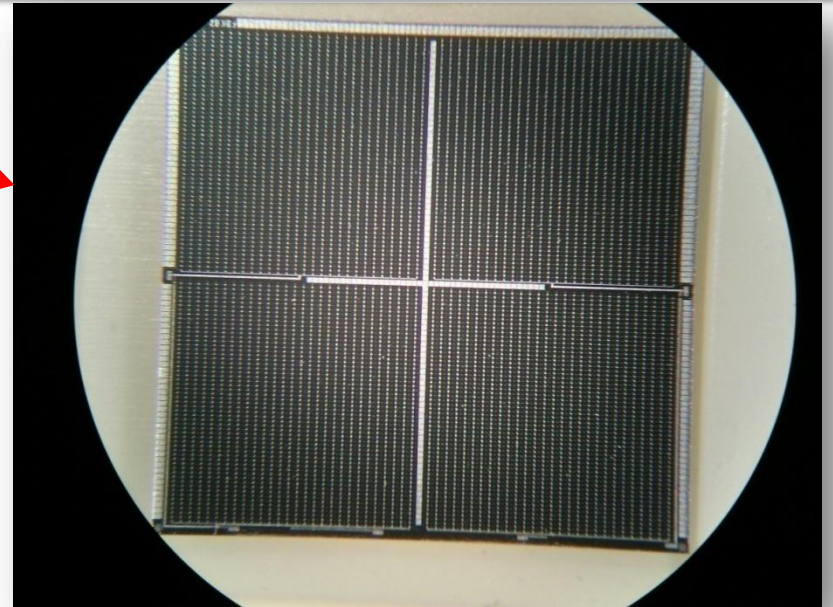
Type	PMT	APD	SiPM
MR compliant	no	yes	yes
ToF compliant	yes	no	yes

2008/09 – large area devices & first productions

Finalized small production for first small animal PET/MR
Produced ~700 fully working arrays

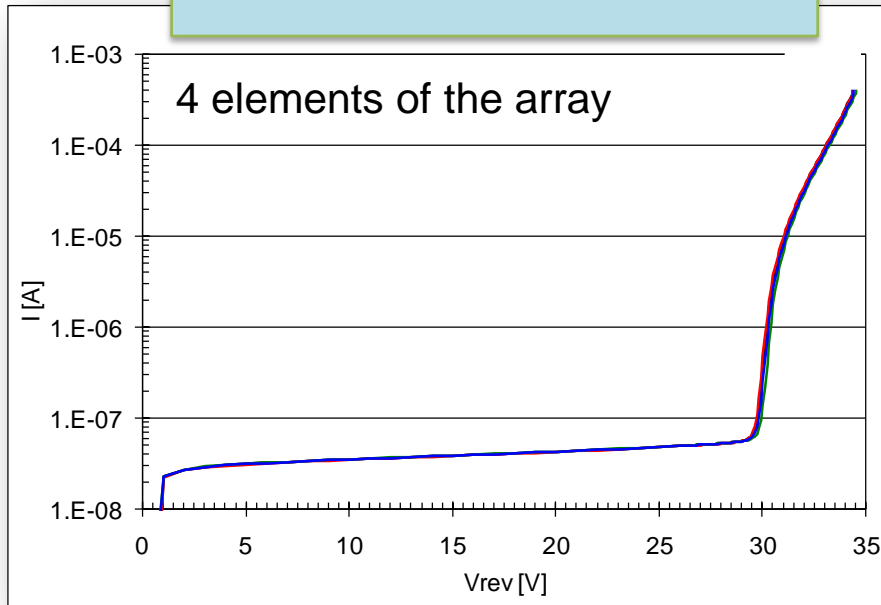


2x2 array of $\sim 4 \times 4 \text{mm}^2$ SiPMs

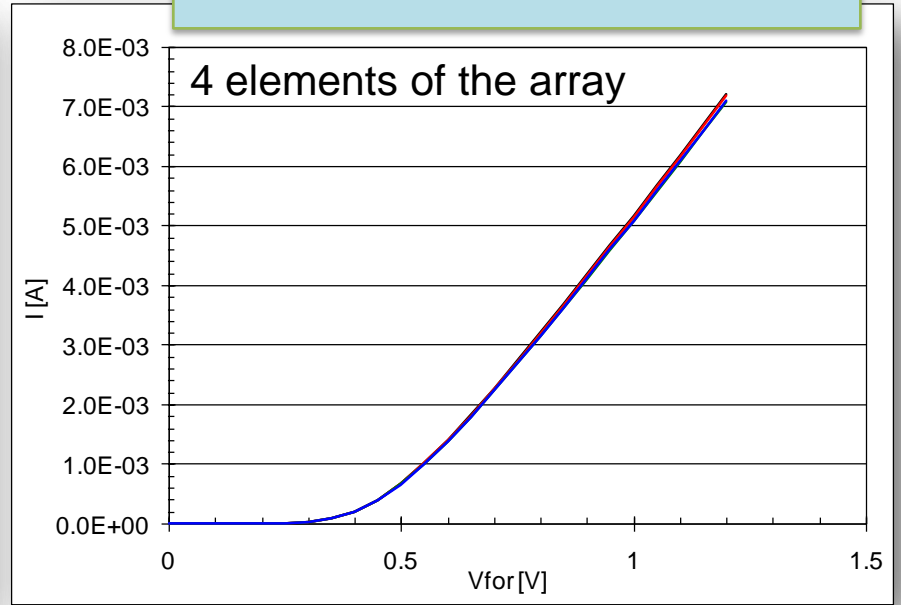


HI SiPM - testing procedure

Reverse charact.



Forward charact.



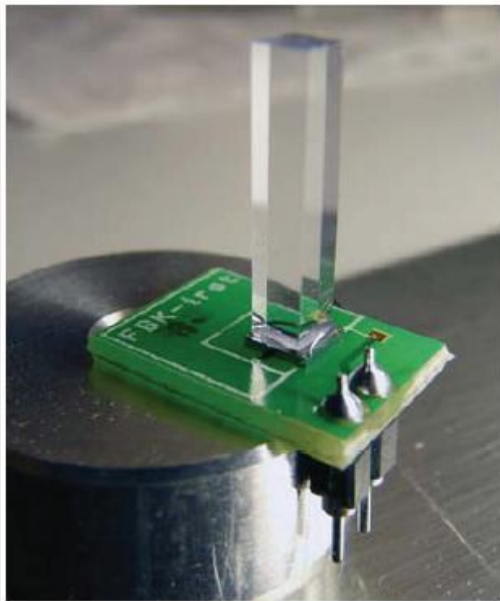
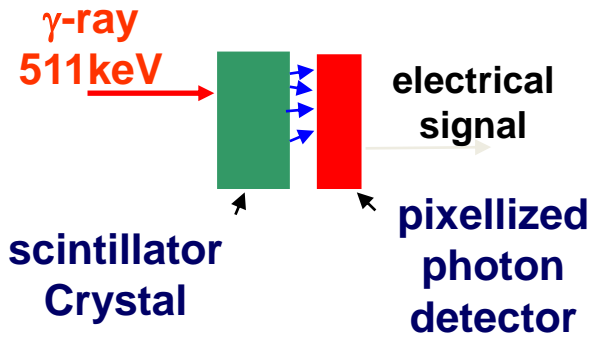
Info we get

- Functionality of the device
- Breakdown voltage
- Dark count estimate

- Functionality of the device
- Resistor value estimate

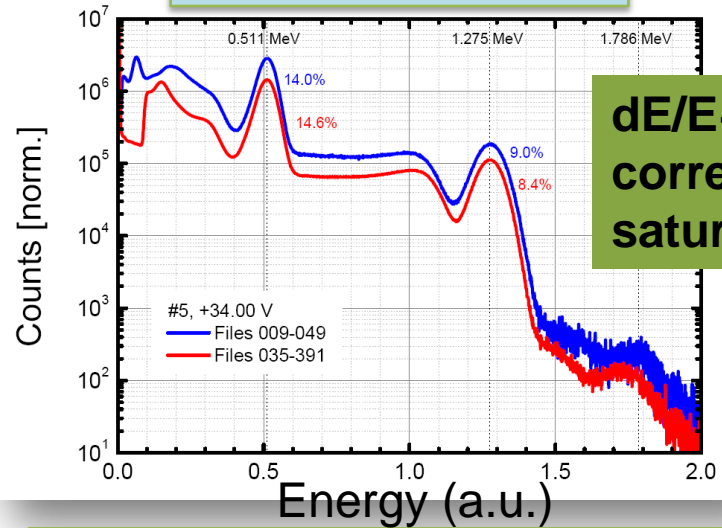
4x4mm² SiPM - 50x50mm² cell

PET application:
SiPM + LYSO



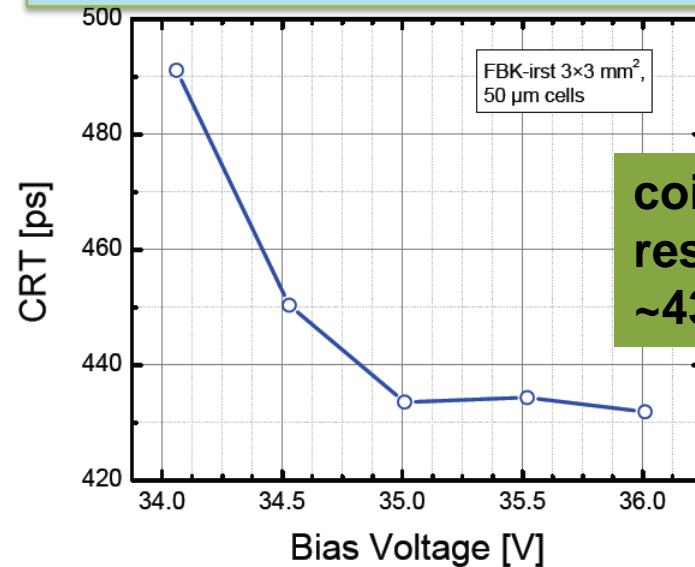
Measurements by Philips Aachen

Energy resolution



**dE/E ~ 14%
corrected for
saturation**

Coincidence time resolution

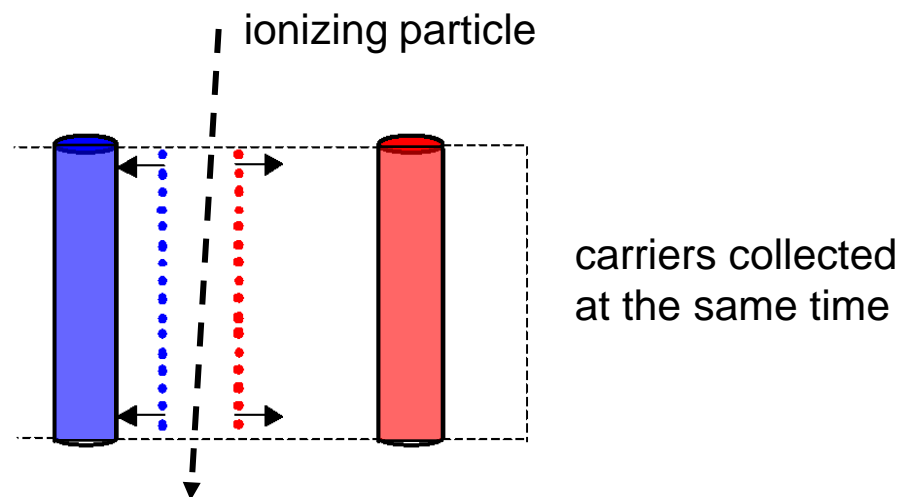
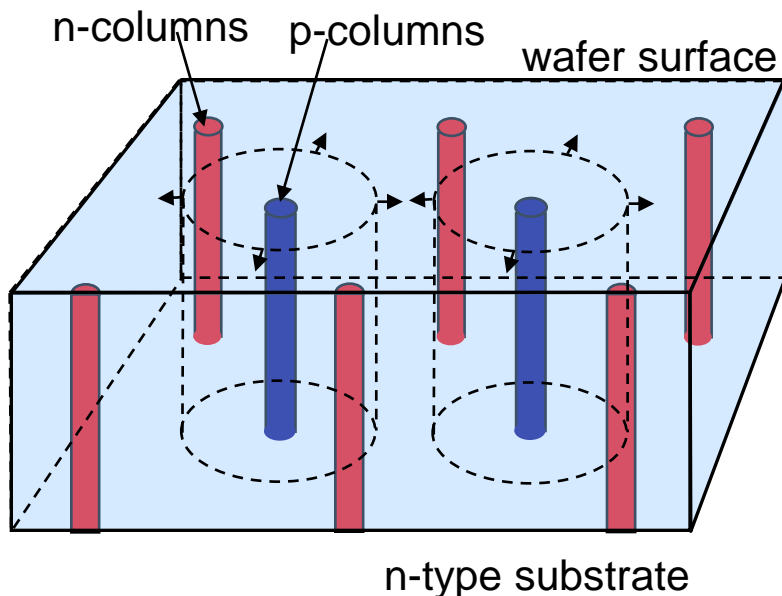


**coincidence
resolution
~430ps**

Silicon 3D

3D detectors - concept

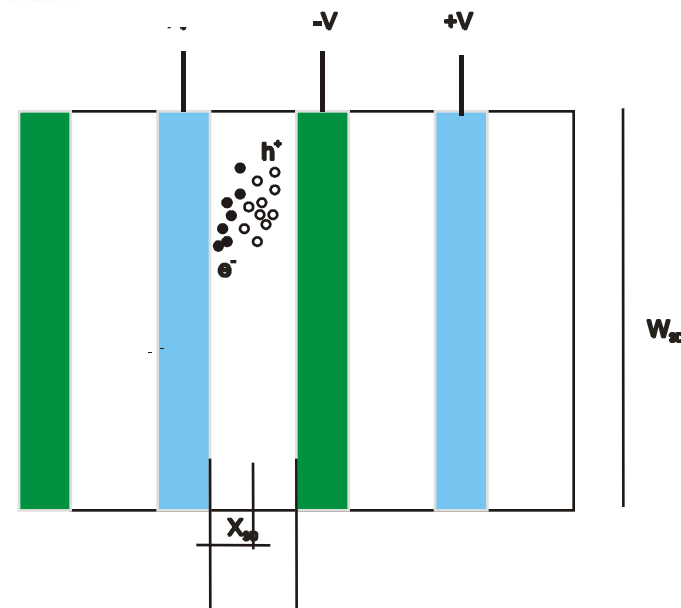
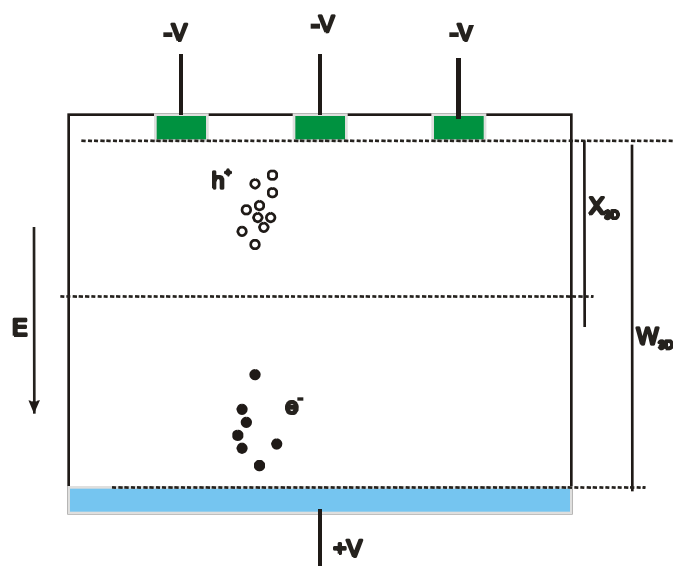
[Parker et al. NIMA395 (1997)]



Distance between n and p electrodes can be made very short

➡ extremely radiation hard detector

3D vs planar



3D features:

- 1) same collected charge as a standard planar with the same thickness;
- 2) lower full depletion voltage (few Volts);
- 3) very short collection time;

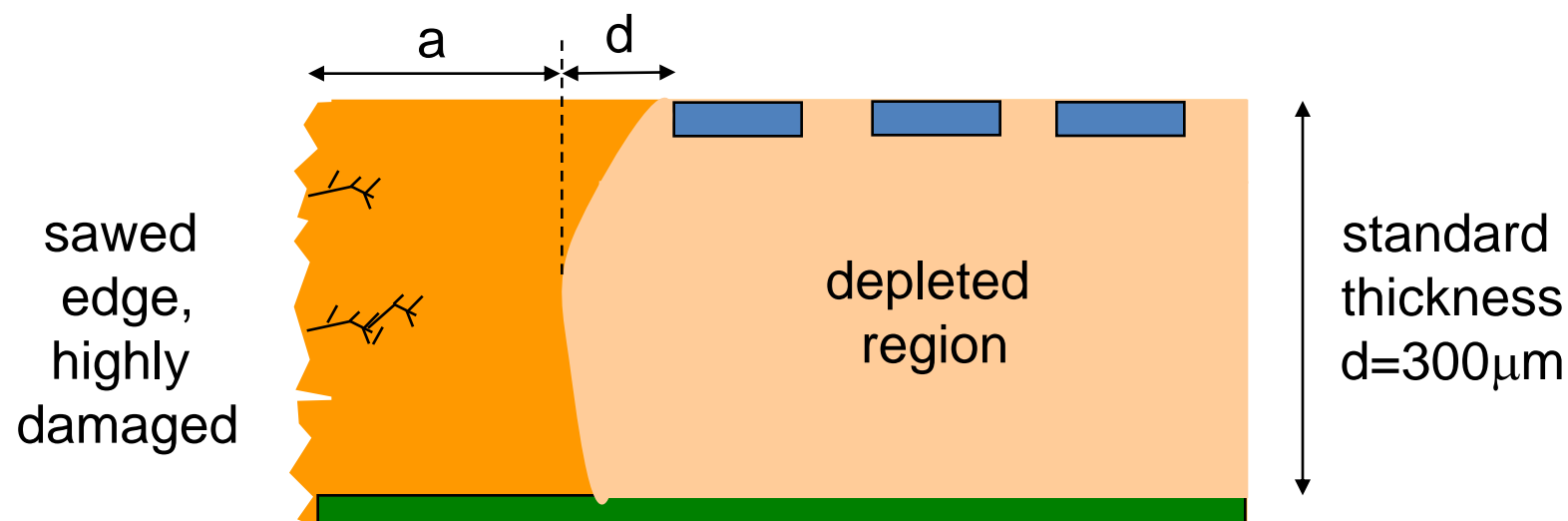
but

- 1) columns are partially dead regions
- 2) Low-field regions exist in between electrodes of same type
- 3) electrode capacitance is higher (noise issues at low t_p)

Other applications of 3d technology : active edge

Problem:

In standard detectors a dead border region must be present:

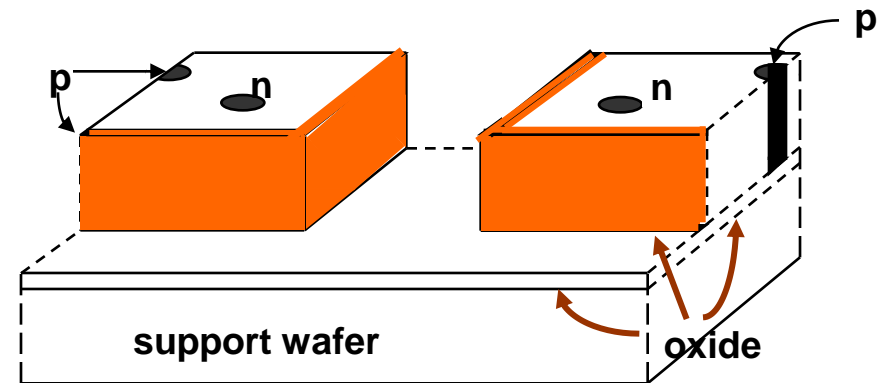
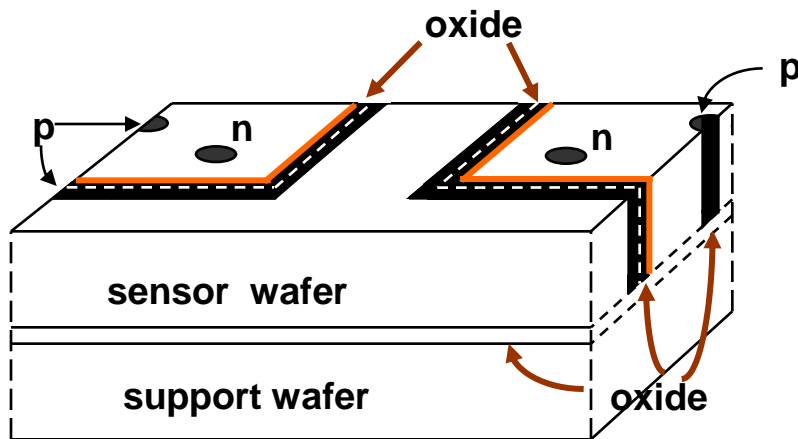


in a good design the cracks must be far from the depletion region,
at least $a=100-200\mu\text{m}$ => **total dead region $a+d=500\mu\text{m}$**

Active edge

How can we limit dead region ?

- ❑ Cut lines not sawed but etched with DRIE & doped



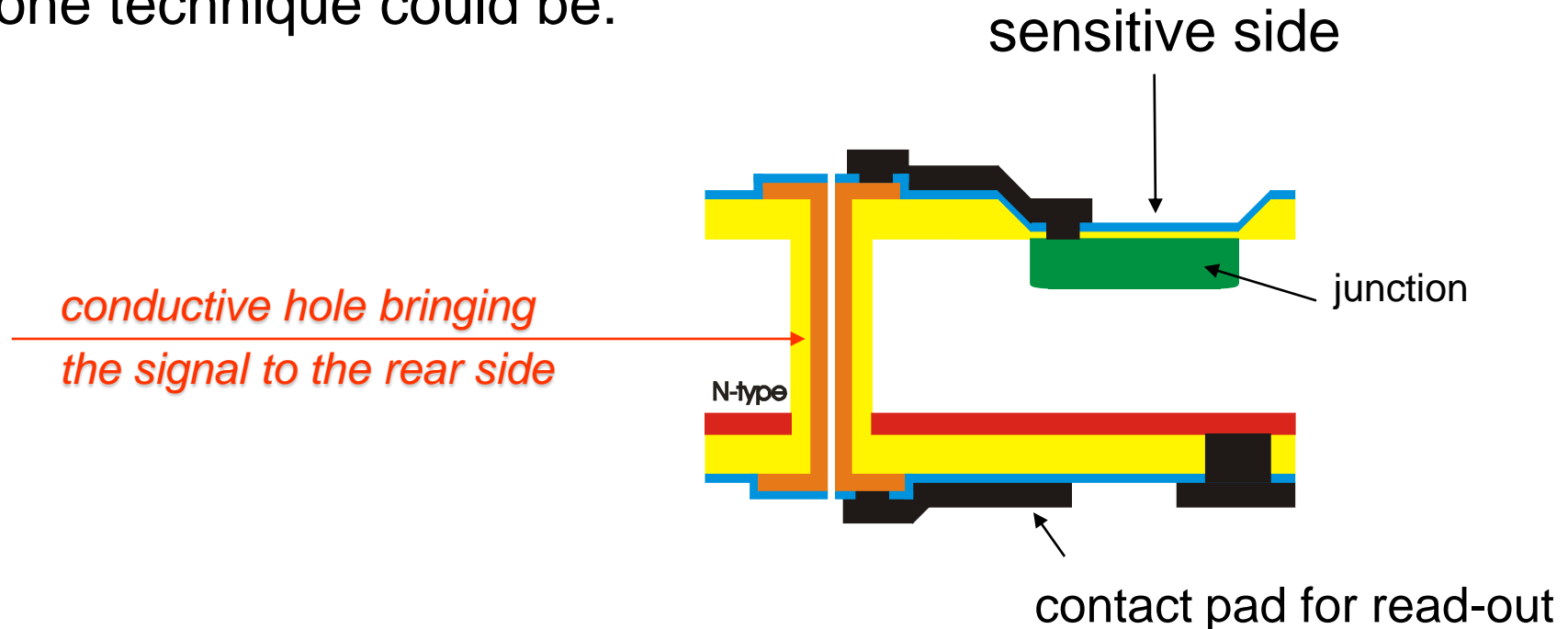
- ❑ Process is more complicated

Need of support wafer → wafer bonding

Other applications of 3d technology: through-wafer interconnects

In light sensors the sensitive side must be clear from obstacles, as can be a read-out chip.

=> one technique could be:



Labs involved in 3D technology

- **Stanford (USA)**

Inventors, state-of-the-art technology (Full 3D with active edge)

But no capability of real production → partnership with SINTEF since 2006

- **FBK-IRST, VTT (Finland), CNM (Spain), BNL (USA)**

Alternative structures with a simplified approach (single type column), moving then to double type column, prototype level

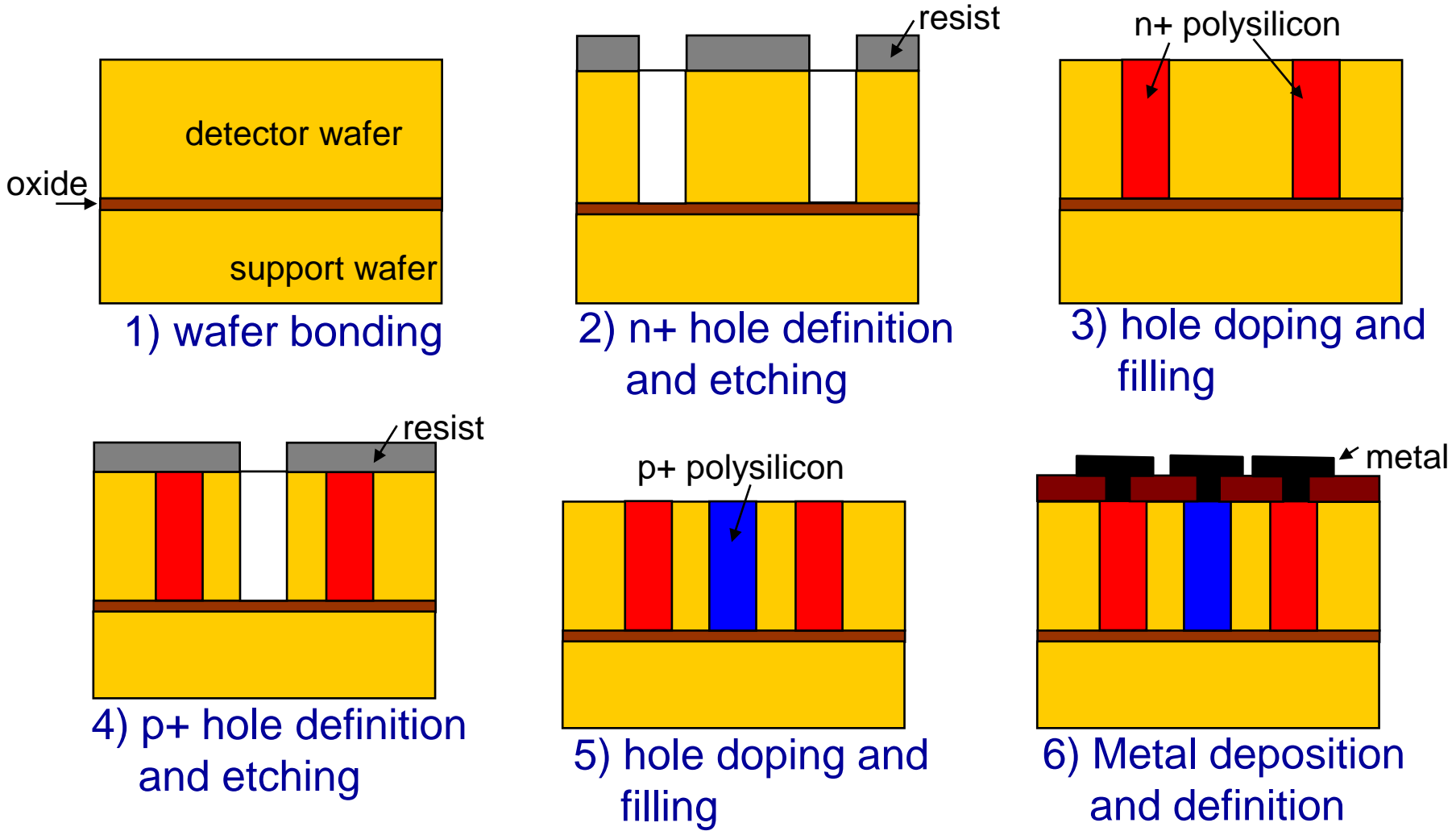
- **ICEMOS (Ireland) in coop. with University of Glasgow (GB)**

Full 3D, with different approach (CMOS based), first results quite disappointing

Since 2006, CERN ATLAS 3D Sensor Collaboration: joint effort to 3D detector optimization in view of SLHC

Stanford detectors: technology

Kenney et al. IEEE TNS, vol. 46, n. 4 (1999)

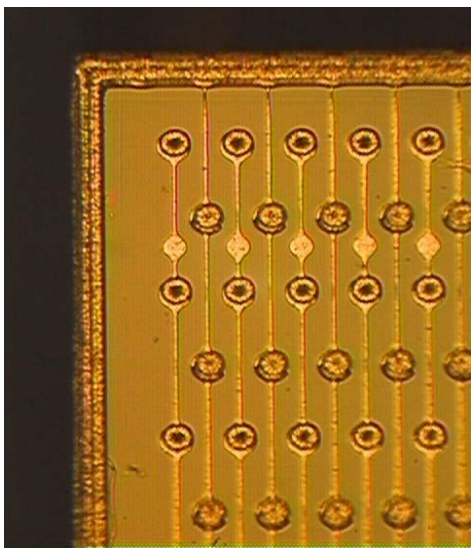
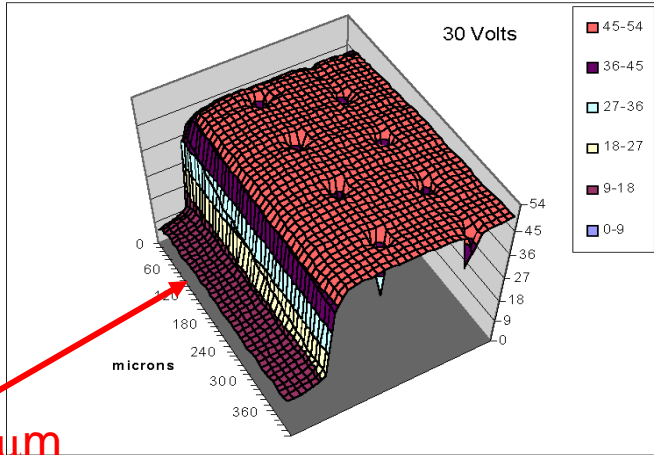


Stanford detectors: Detector inefficiencies

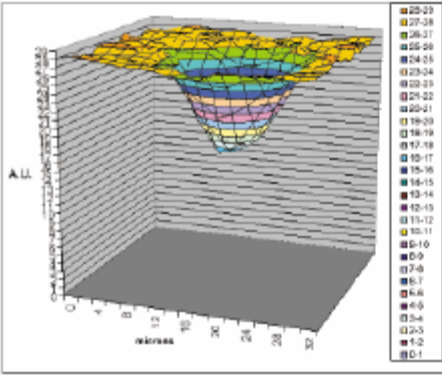
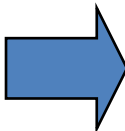
X-ray microbeam

Scanning the beam over the detector surface and measuring the signal charge it is possible to evidence the inefficient regions

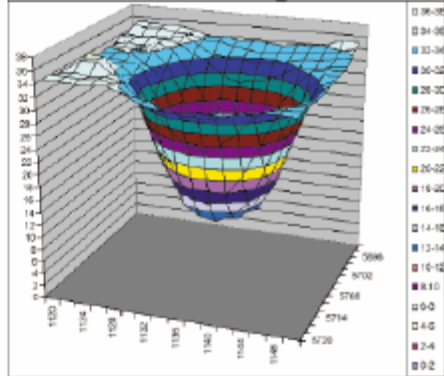
10-90% < 5μm



Electrode response using 12KeV X-ray beam (ALS), beam size ~ 2μm



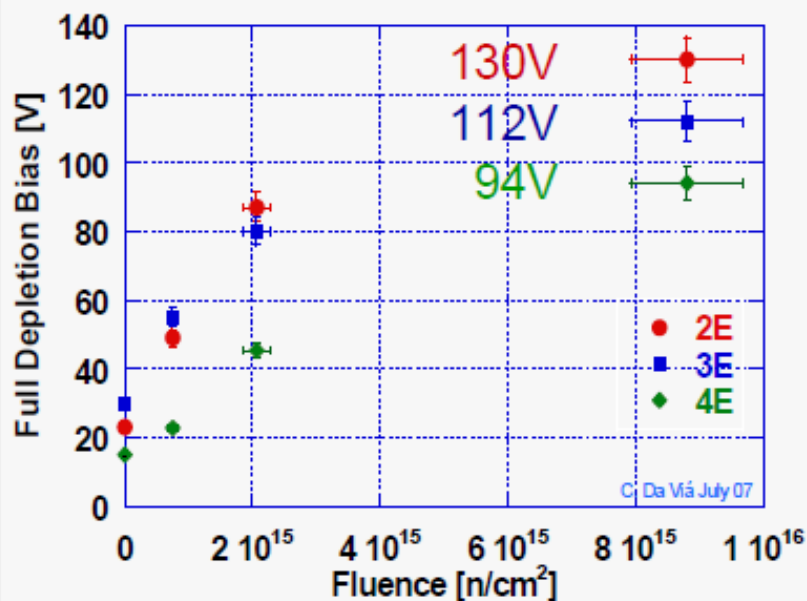
N – Electrode
Signal Reduction 43%



P – Electrode
Signal Reduction 66%

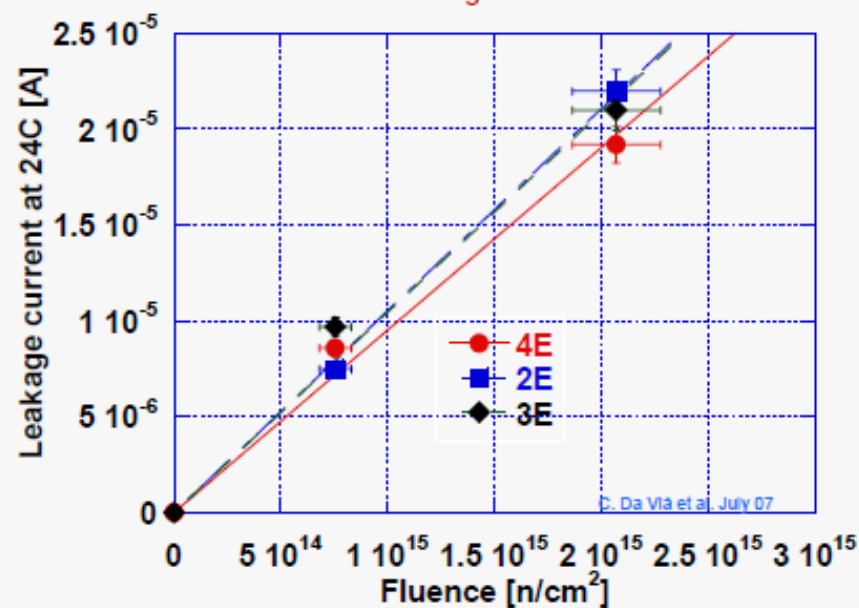
Stanford detectors: Radiation hardness

Voltage for full depletion



RT Leakage current at full depletion

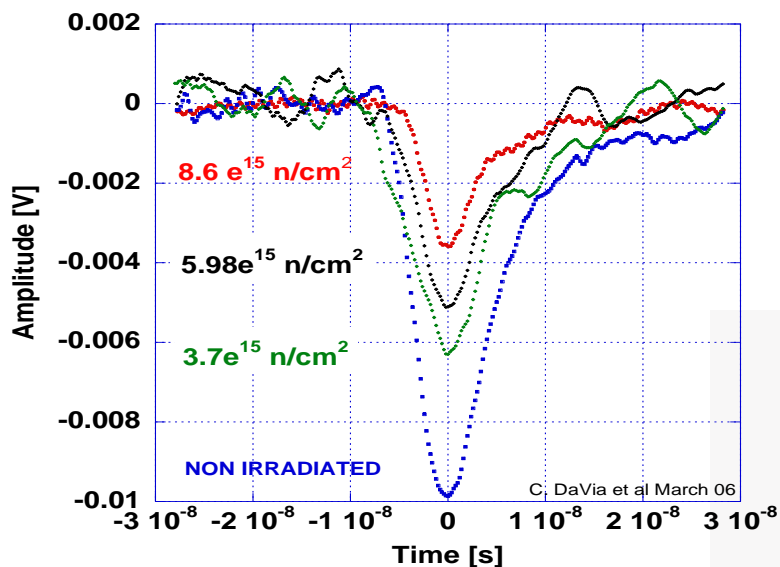
Partial beneficial annealing



4E	Fluence [n/cm ²]	I _{FD} at 24°C [A]	Alpha [A/cm]	V _{FD} [V]	Max ampl. [mV]
Non Irrad.	0	--	--	15	124
samp1	7.55e+14	8.58e-06	6.3e-17	22	124
samp2	2.07e+15	19.2e-06	5.1e-17	45	120
samp3	8.81e+15	80.0e-06	4.3e-17	94	82

Stanford detectors: Charge collection efficiency

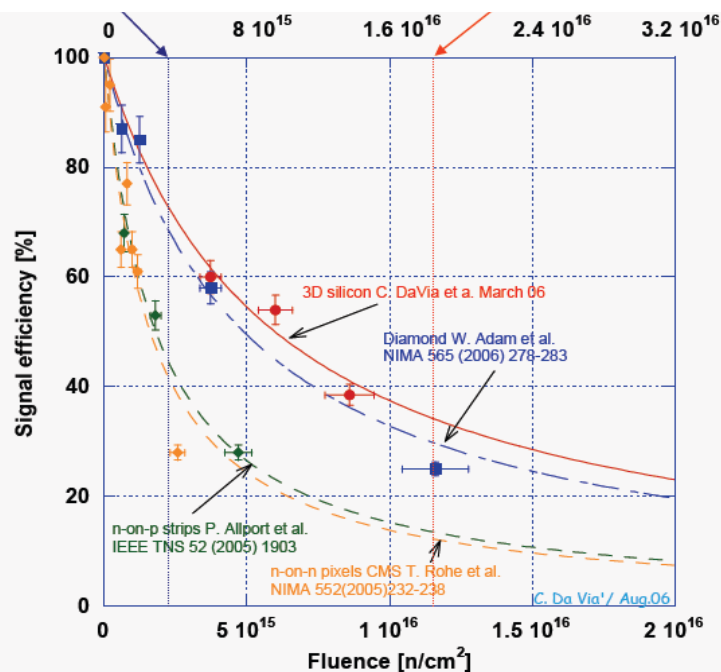
Cinzia Da Via' - VSTD6 -- September 2006



Increasing the irradiation level the signal decreases because of charge trapping

Charge collection efficiency.

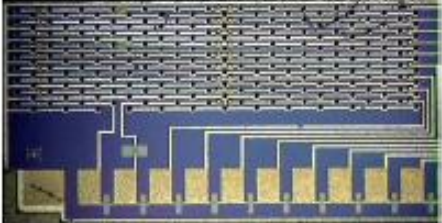
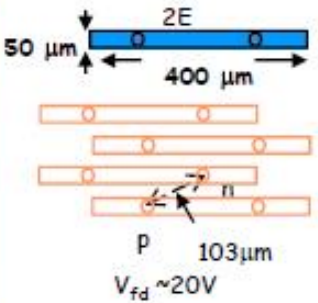
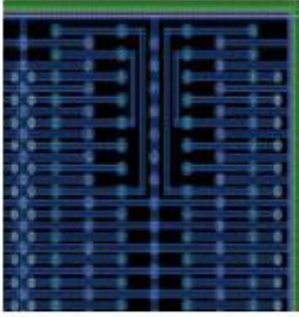
3D (red line) behave much better than standard planar (orange and green) and comparable with diamond detectors



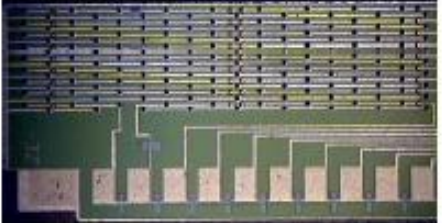
ATLAS 3D pixels

Design and fabrication by:
 J. Hasi, Manchester
 C. Kenney, MBC at CIS-Stanford

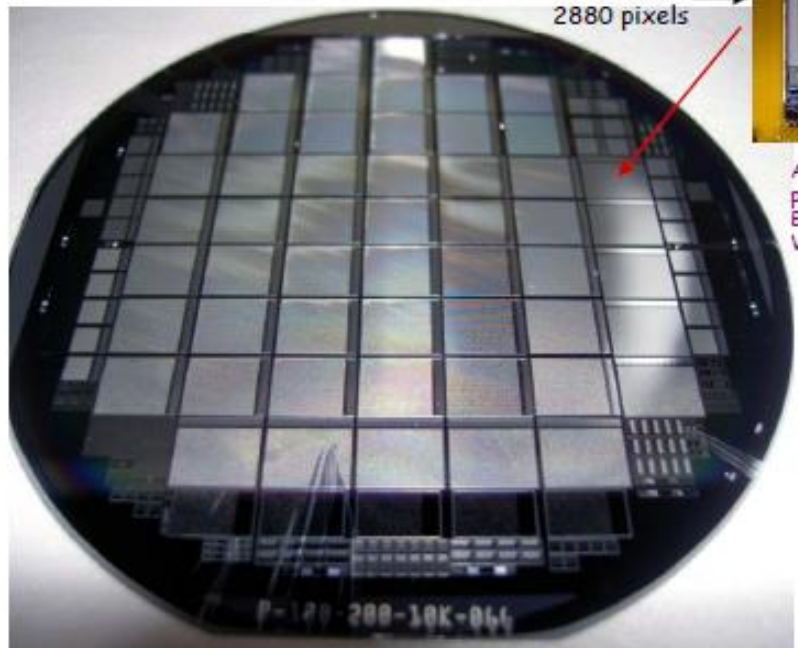
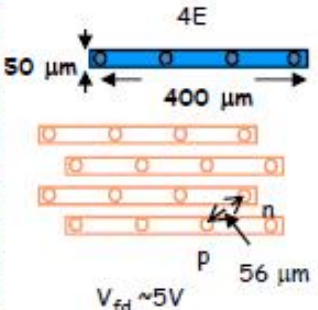
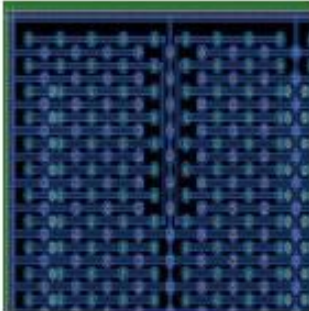
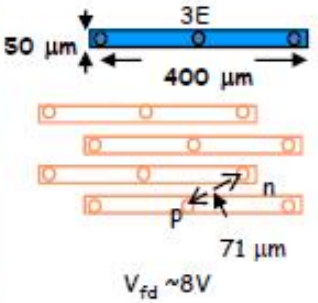
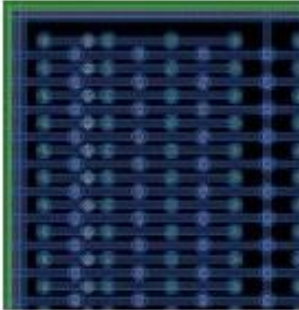
Thickness <math>< 210 \mu\text{m}</math>
 p-type substrate $12\text{k}\Omega\text{cm}</math>$



Baby-2E



Baby-3E



10 wafers being competed. Yield ~ 80% (1 wafer)

ATLAS pixel chip
 7.2 x 8 mm²
 2880 pixels

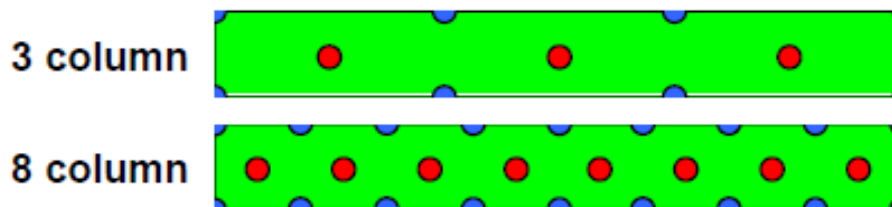


Atlas chip picture from Bekerle Vertex03

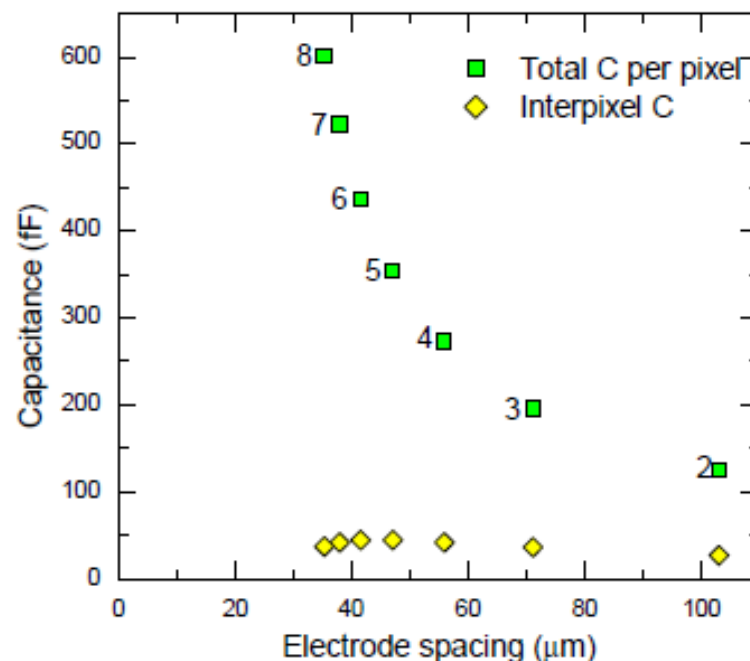
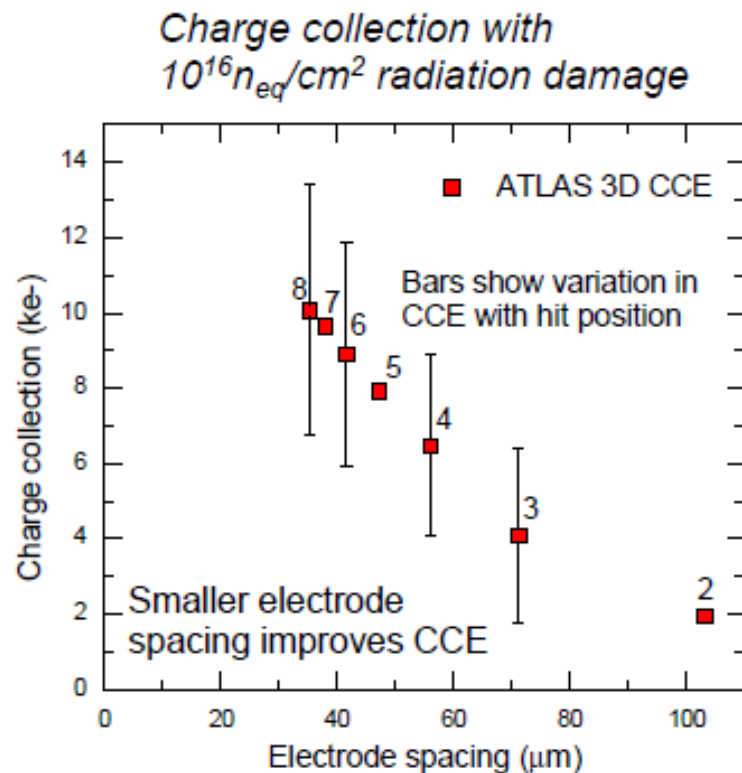
Pixel capacitance

- ATLAS pixel is $400\mu\text{m} \times 50\mu\text{m}$
 - Different layouts available
 - Trade-offs between V_{dep} , CCE, capacitance, column area...

D. Pennicard et al., *Nucl. Instr. Meth. A* 592 (2008) 16

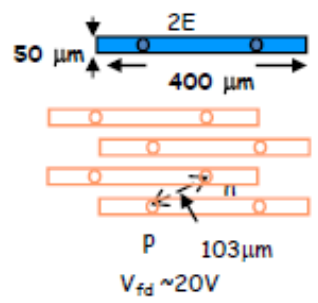


Capacitance at each pixel

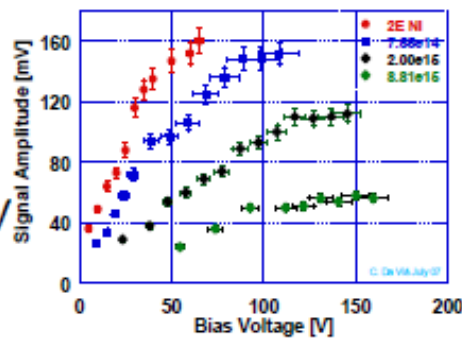


Radiation hardness

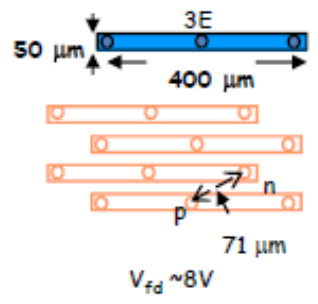
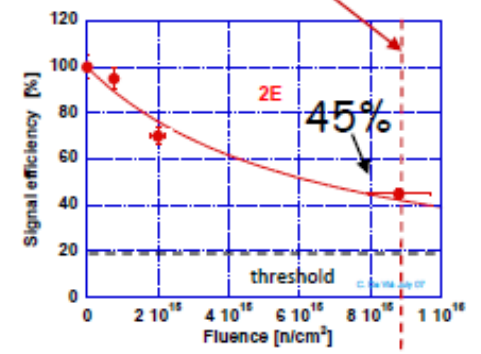
Irradiation and measurements performed in Prague
 C. Da Viá, T. Slaviceck, V. Linhart, P. Bem, S. Parker,
 S. Pospisil, S. Watts (process J. Hasi, C. Kenney)



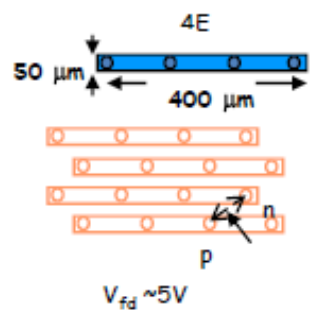
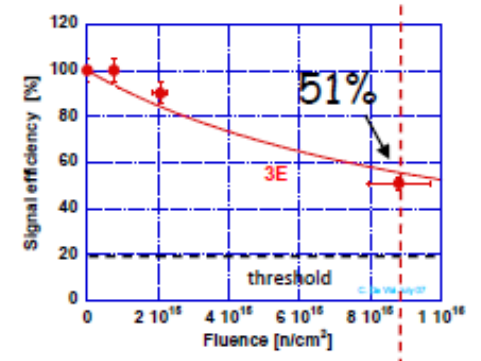
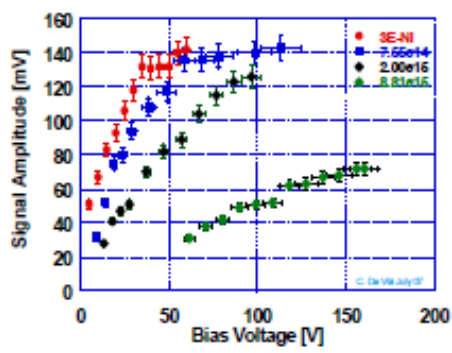
2E
 9000e⁻
 V_b ~ 130V



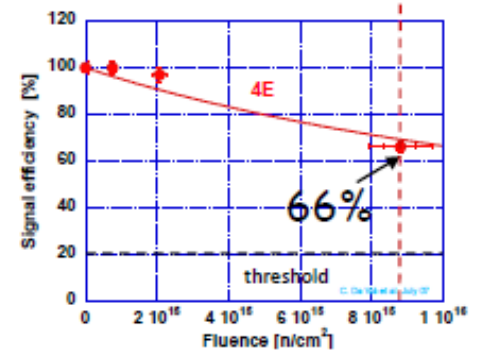
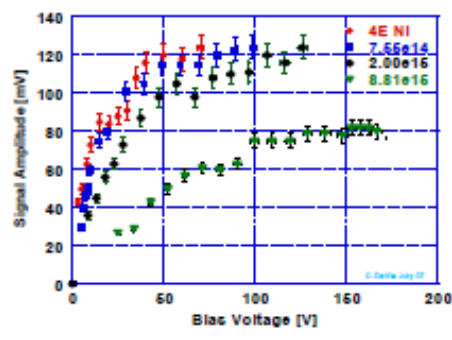
8.81×10¹⁵ n/cm²
 1.73×10¹⁶ p/cm²



3E
 10200e⁻
 V_b ~ 112V



4E
 13200e⁻
 V_b ~ 94V

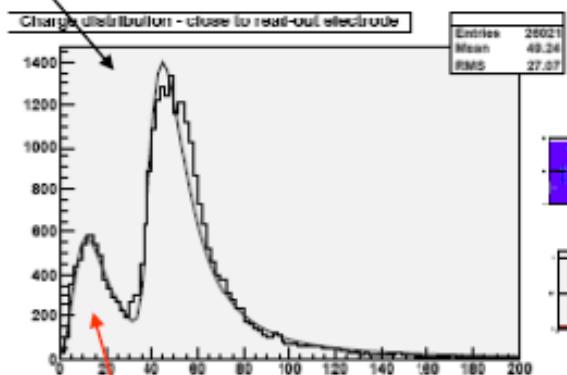
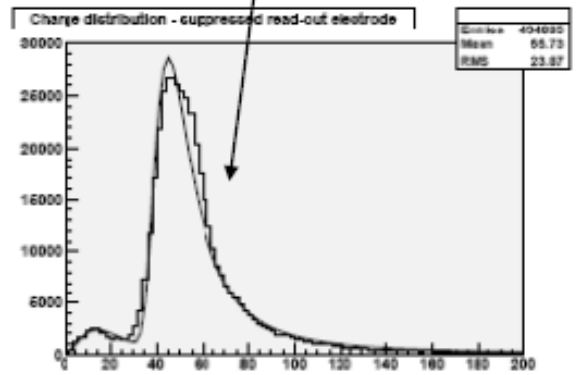
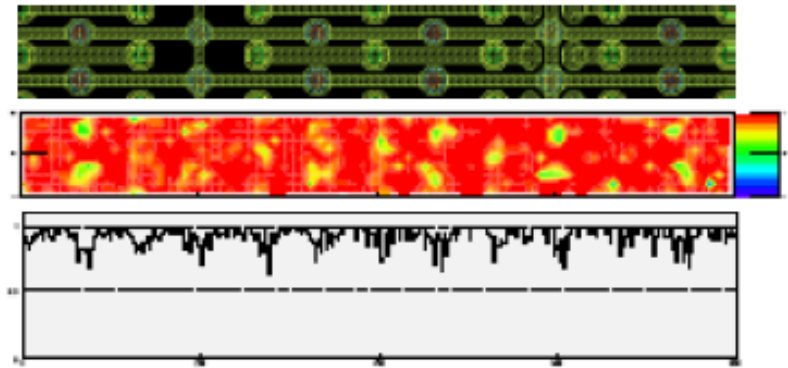
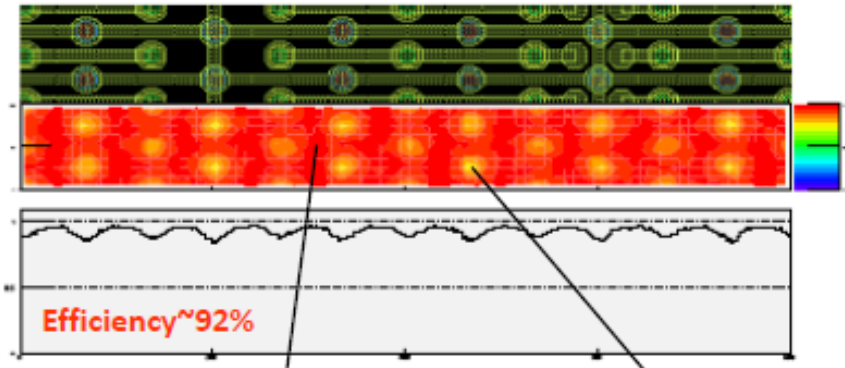


Preliminary results: test beam June 2008

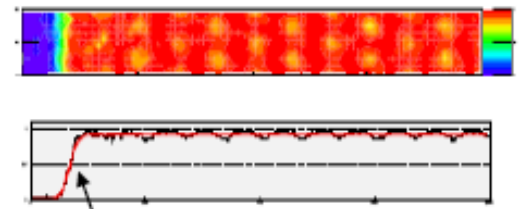
Ian McGill
Beniamino Di Girolamo
Bonn University with IZM Bump-bonding and telescope
E. Bolle, B. Buttler, C. Da Via, O. Dorholt, S. Fazio,
H. Gjerdal, J. Hasi, A. La Rosa, C. Kenney, D. Miller,
C. Young, V. Linhart, H. Pernegger, T. Slavicec, K. Sjobak,
M. Tomasek, S. Watts

3E-40V

3E-10V



Edge response

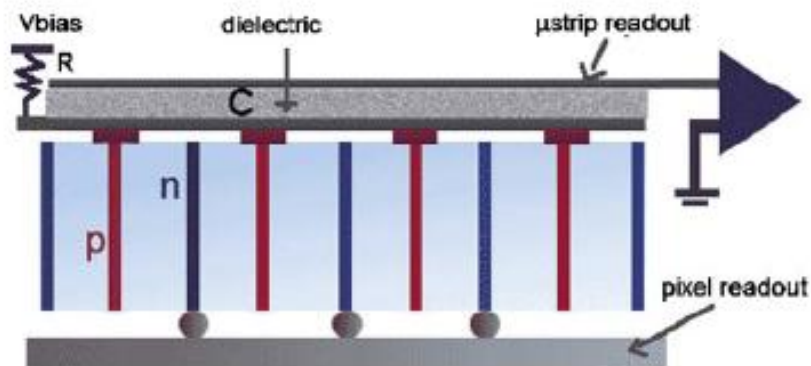


10-90% ~25µm
Analysis ongoing

Electrode efficiency ~27%

Data presented at IEEE-NSS08 by O. Rohne, Olso

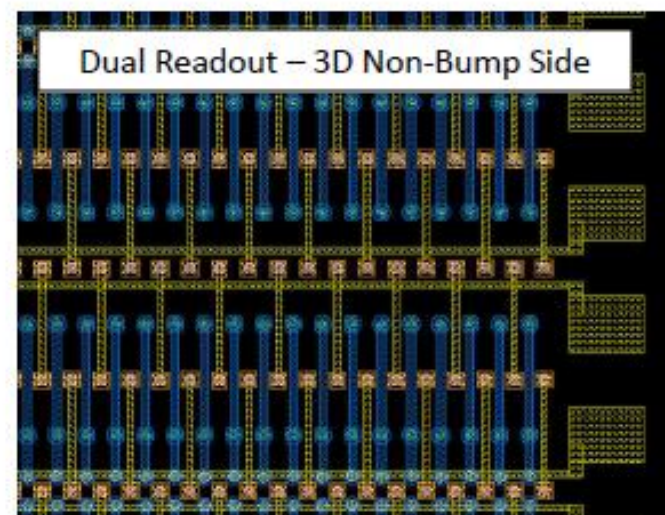
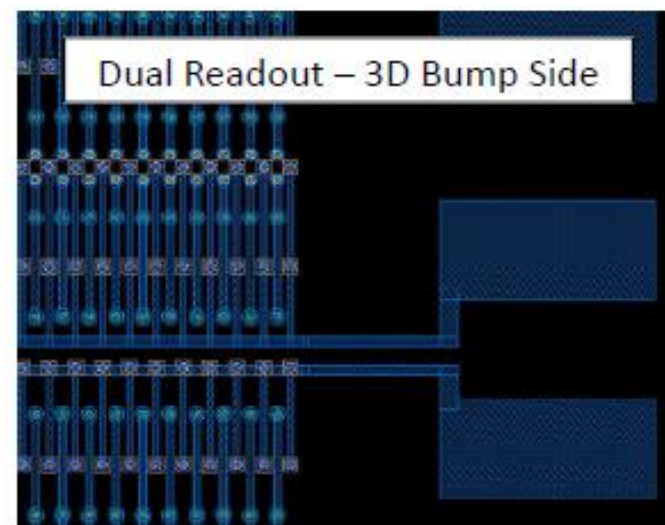
Dual read-out



C. Da Via et al., "Dual readout - strip/pixel systems",
NIM A594, pp. 7-12 (2008).

Devices being
presently processed
Prototypes available in
spring-summer09.
Might be used for
trigger at AtlasFP

From Kenney US Atlas Upgrade meeting
September 08



3d detectors @ FBK

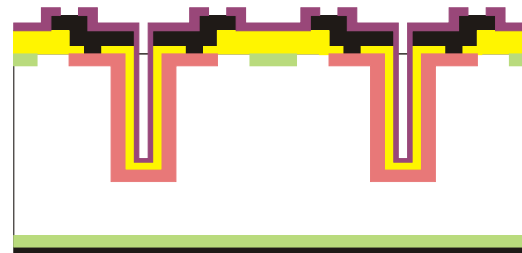
FBK is developing the technology for the production of 3D detectors in a three phases program:

SINGLE TYPE COLUMNS

Simple fabrication process

- holes not etched all through the wafer
- Single side process

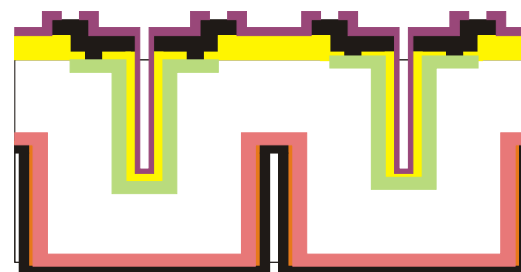
Collection mechanism not very efficient



DOUBLE TYPE COLUMNS

Performance enhancement with acceptable process complication

- holes not etched all through the wafer
- Double side process
- p-on-n an n-on-p



FULL 3D

holes etched all through the wafer

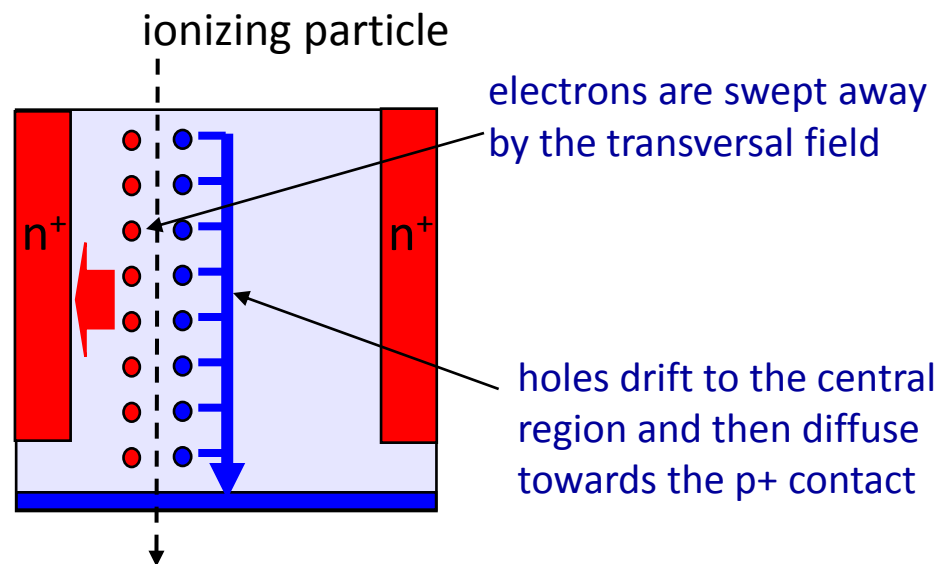
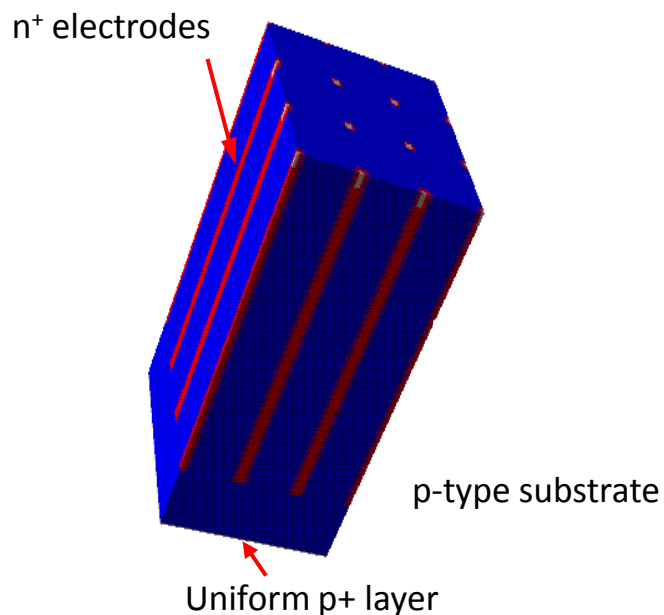
Single or double side process

EDGELESS 3D DETECTORS

Single-Type-Column 3D detectors

[C. Piemonte et al NIMA 541 (2005)]

...on the way to a fully 3D device: 3D-STC



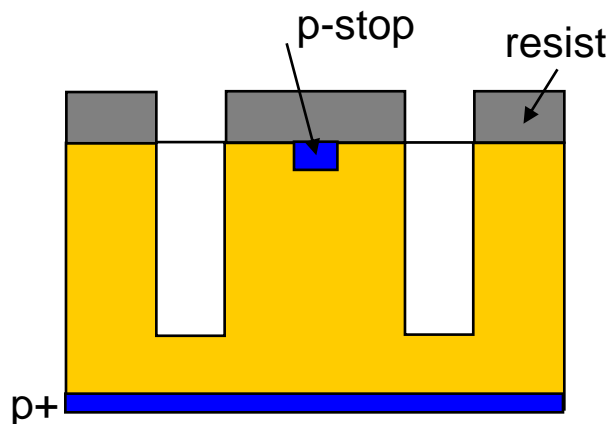
Fabrication process is much simpler:

- column etching and doping performed only once
- holes not etched all through the wafer

...BUT

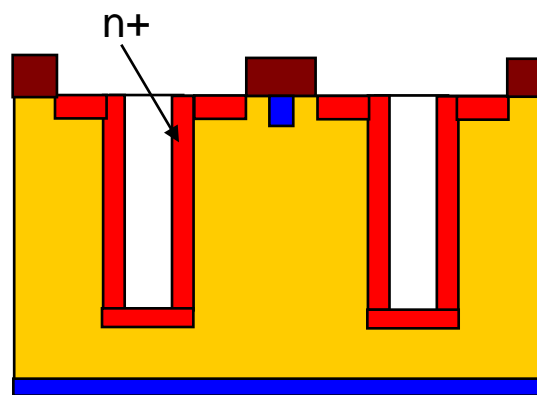
Collection mechanism
is not very efficient!

3D-STC detectors - technology



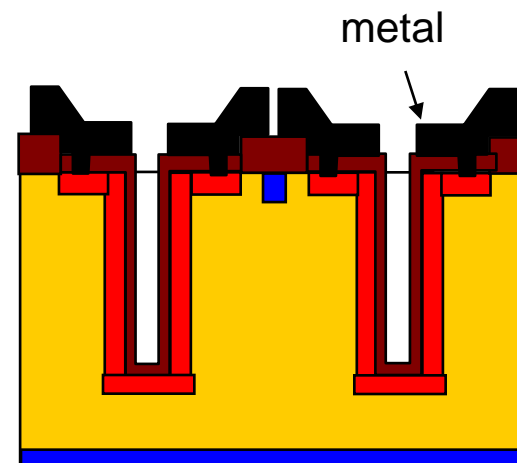
1) n+ hole definition
and etching

Holes:
200 μ m depth with a
radius of \sim 5 μ m



2) hole doping

Doping by simple P
diffusion or by
P-doped poly-Si
deposition



3) Metal deposition
and definition

Holes are **partially** filled
with thermal oxide
or TEOS.

Contact only at the top.

Punti chiave per la realizzazione di un 3D

- **DRIE**
 - AD ORA È L'UNICA TECNOLOGIA UTILIZZABILE PER LA REALIZZAZIONE DI FORI PROFONDI
 - CHE TIPO DI MASCHERATURA ?
 - ASPECT RATIO ?
- **DROGAGGIO TRAMITE SORGENTI A STATO SOLIDO**
 - NON SI PUÒ PENSARE DI IMPIANTARE IN UN FORO PROFONDO
- **RIEMPIMENTO CON POLISILICIO**
 - SE DA BUONI RISULTATI IN TERMINI DI RIDUZIONE DELL'AREA MORTA SICURAMENTE COMPLICA DECISAMENTE IL PROCESSO
 - RIEMPIRE IL FORO $10 \text{ DIAMETRO} = 5 \text{ MICRON DI POLY}$
 - NECESSITA DI CMP
- **WAFER BONDING**
 - FONDAMENTALE PER EDGLESS
 - IL PROBLEMA È STACCARE LA FETTA DI SUPPORTO
- **LITHO IN PRESENZA DI FORI**
 - IN GENERALE LA GESTIONE DEI FORI È UN PROBLEMA "PRATICO"
 - RESISTENZA MECCANICA

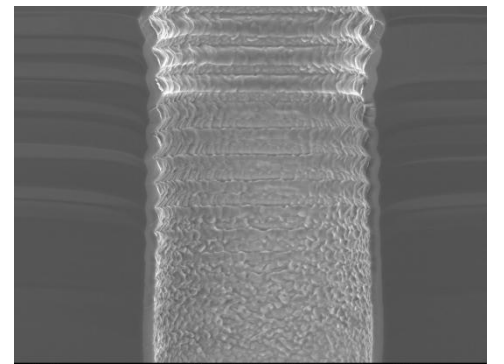
Deep Reactive Ion Etching

Deep reactive-ion etching (DRIE) is a highly anisotropic etch process

Aspect ratio of 20:1 or more.

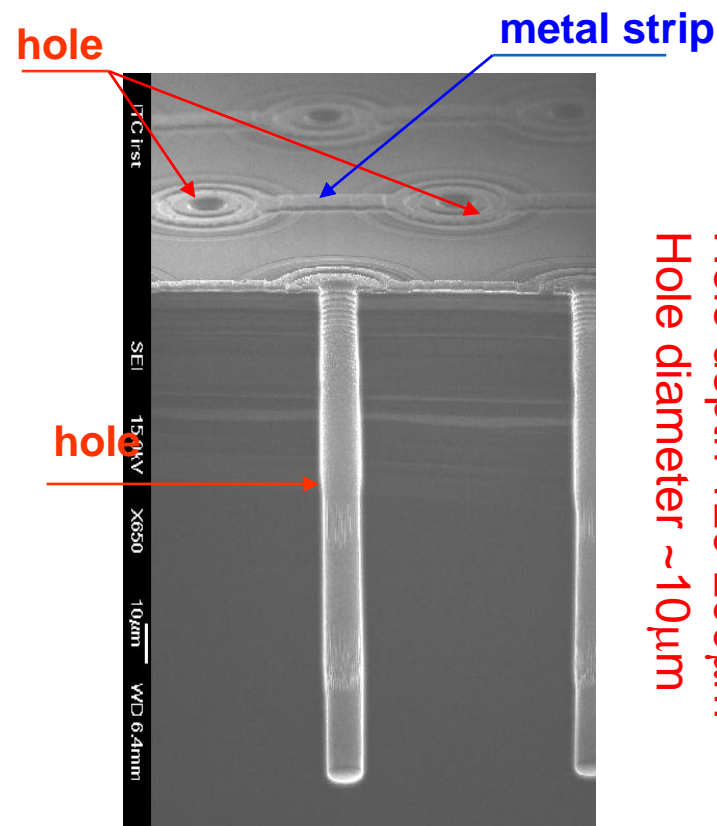
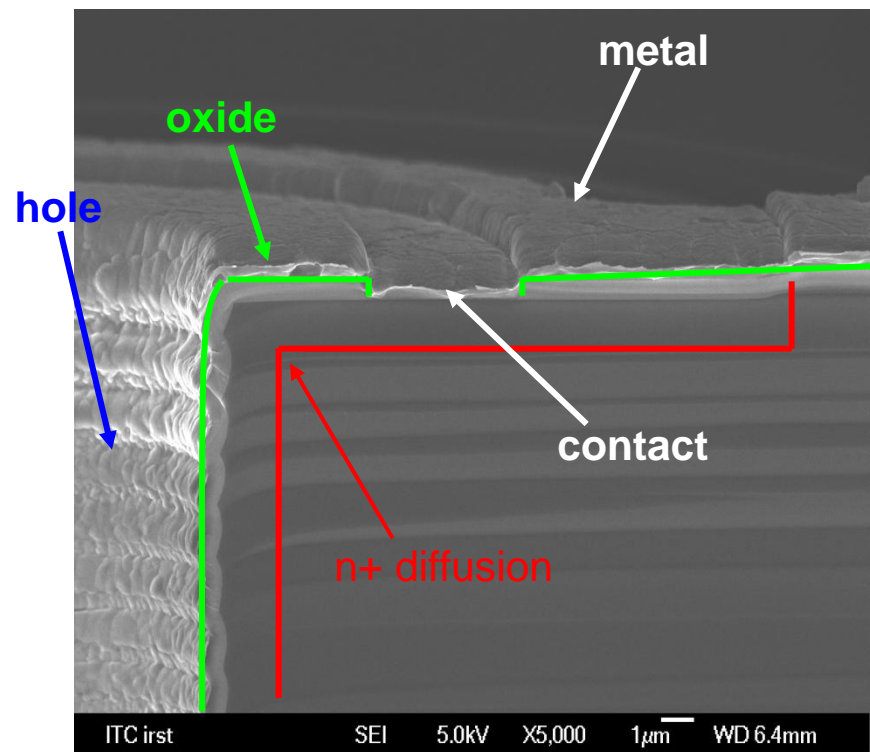
The Bosch process alternates repeatedly between two modes to achieve nearly vertical structures.

1. A standard, nearly isotropic plasma etch
2. Deposition of a chemically inert passivation layer



3D-STC detectors - FBK technology

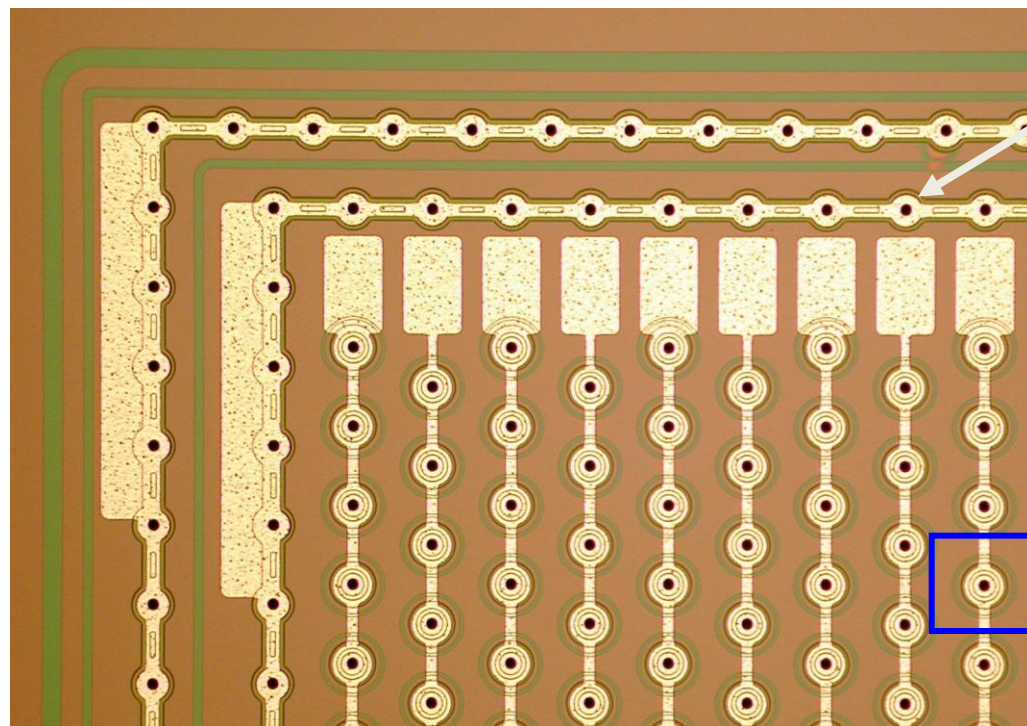
- Hole etching with Deep-RIE technology
- Wide superficial n+ diffusion in which the contact is located
- Passivation of holes with oxide



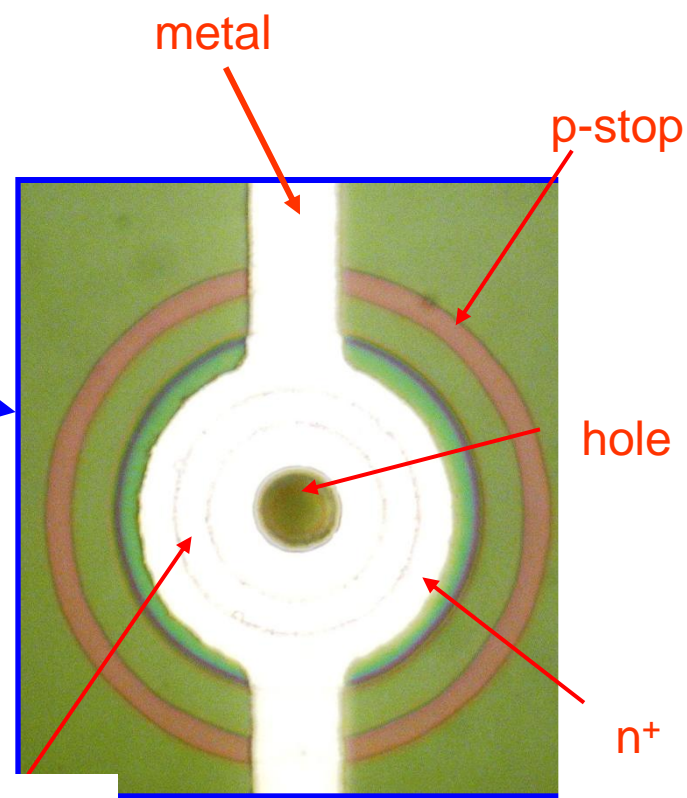
Hole depth 120-200µm
Hole diameter ~10µm

- Si High Resistivity, p-type, <100>
- Surface isolation: p-stop or p-spray
- Holes are "empty"

3D-STC detectors - Strip detectors



Inner guard ring (bias line)

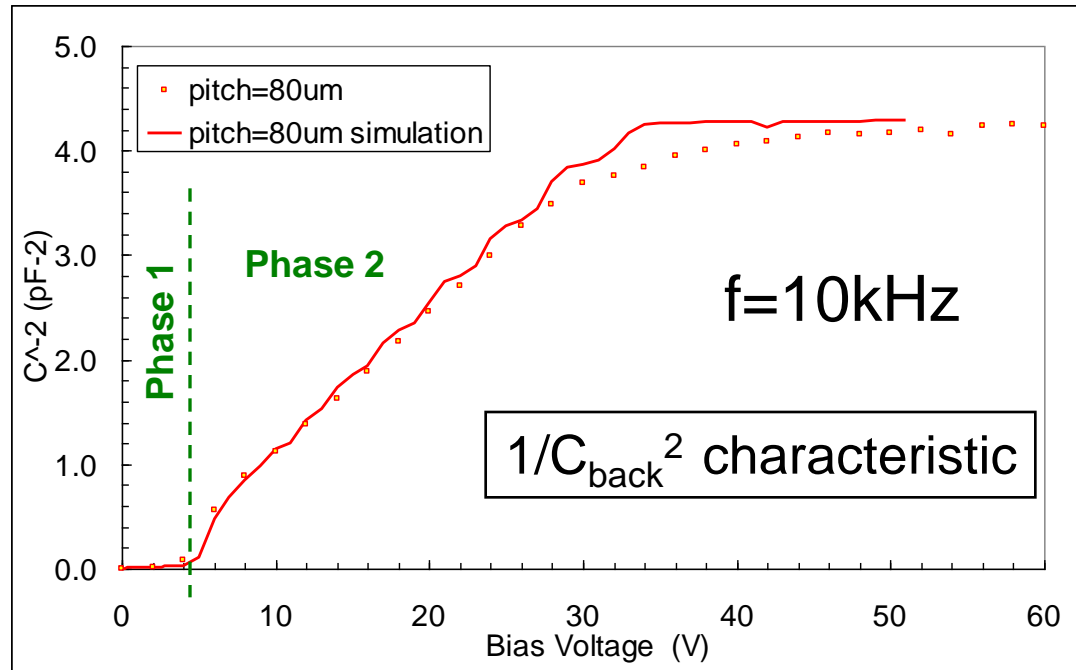
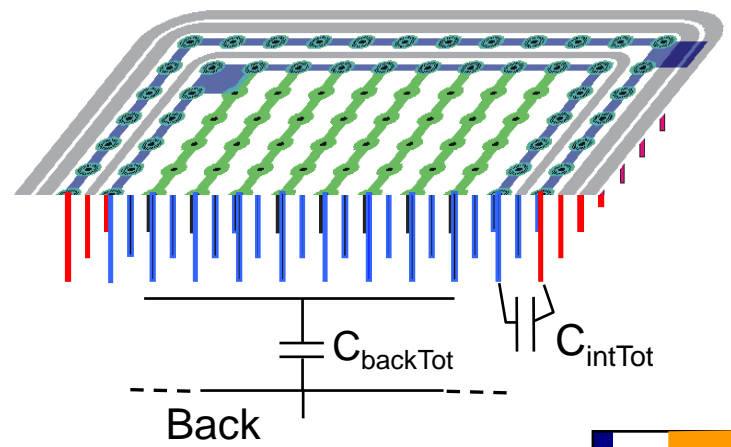


Contact
opening

Different strip-detector layouts:

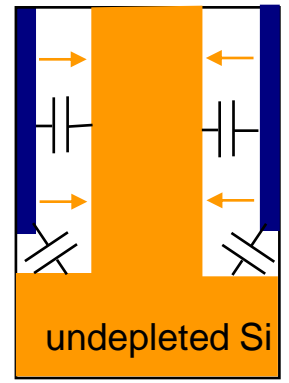
- Number of columns from 12000 to 15000
- Inter-columns pitch 80-100 μm
- Holes \varnothing 6 or 10 μm

Full depletion evaluation from 3D diode capacitance



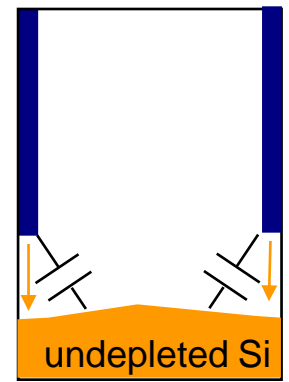
Phase 1

- high C_{back}
- ~ zero C_{int}



Phase 2

- max C_{int}
- slowly dec. C_{back}

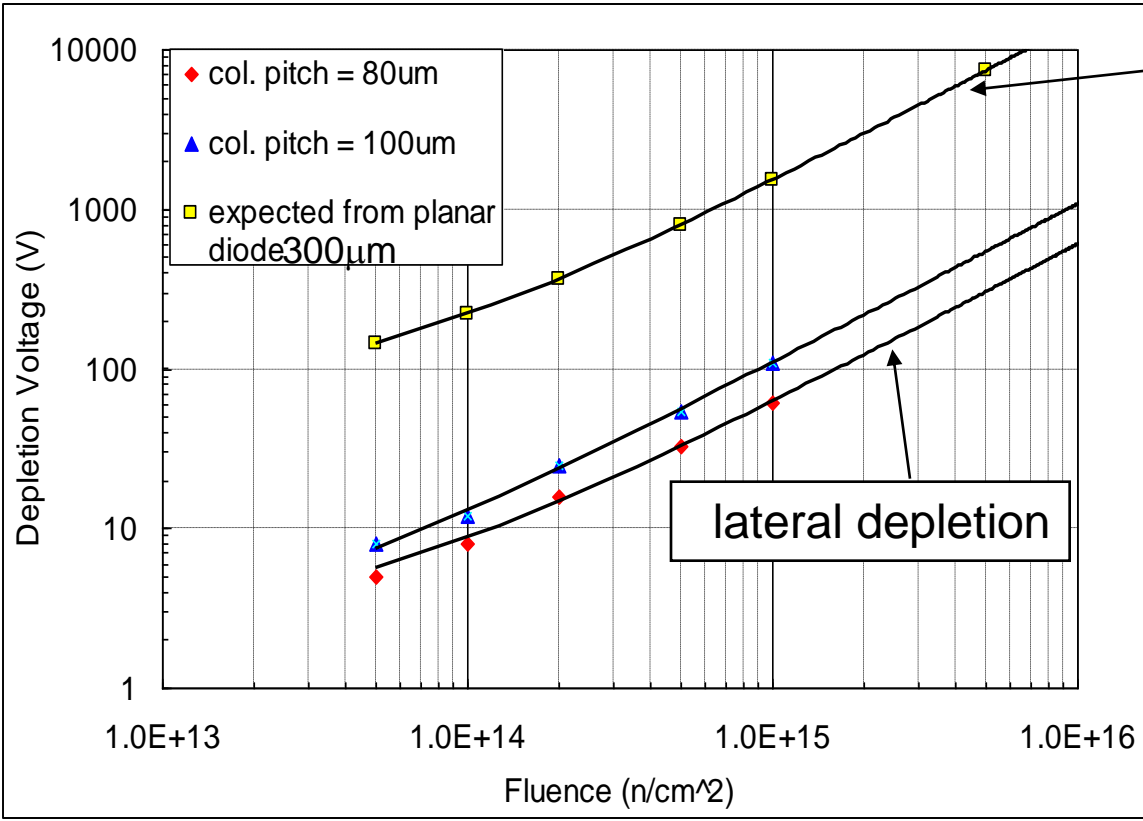


From $1/C^2$ curves one can determine:

- full depletion between columns (in this case ~5V for 80 μm col. pitch)
- full depletion of the bottom region (~35V for column depth of 150 μm)

Depletion voltage after irradiation

(JSI Ljubljana)



$$\Delta N_{\text{eff}} = \beta * \Phi \quad (*)$$

$$\beta = 0.021 \text{ cm}^{-1}$$

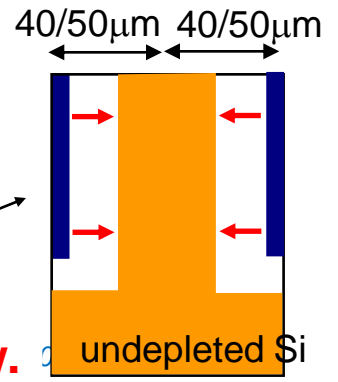
see V. Cindro's talk
 at 8th RD50 workshop:
<http://rd50.web.cern.ch/rd50/>

Simulating the full lateral depletion voltage with N_{sub} estimated from equation (*) we obtain values comparable with those reported on the plot.

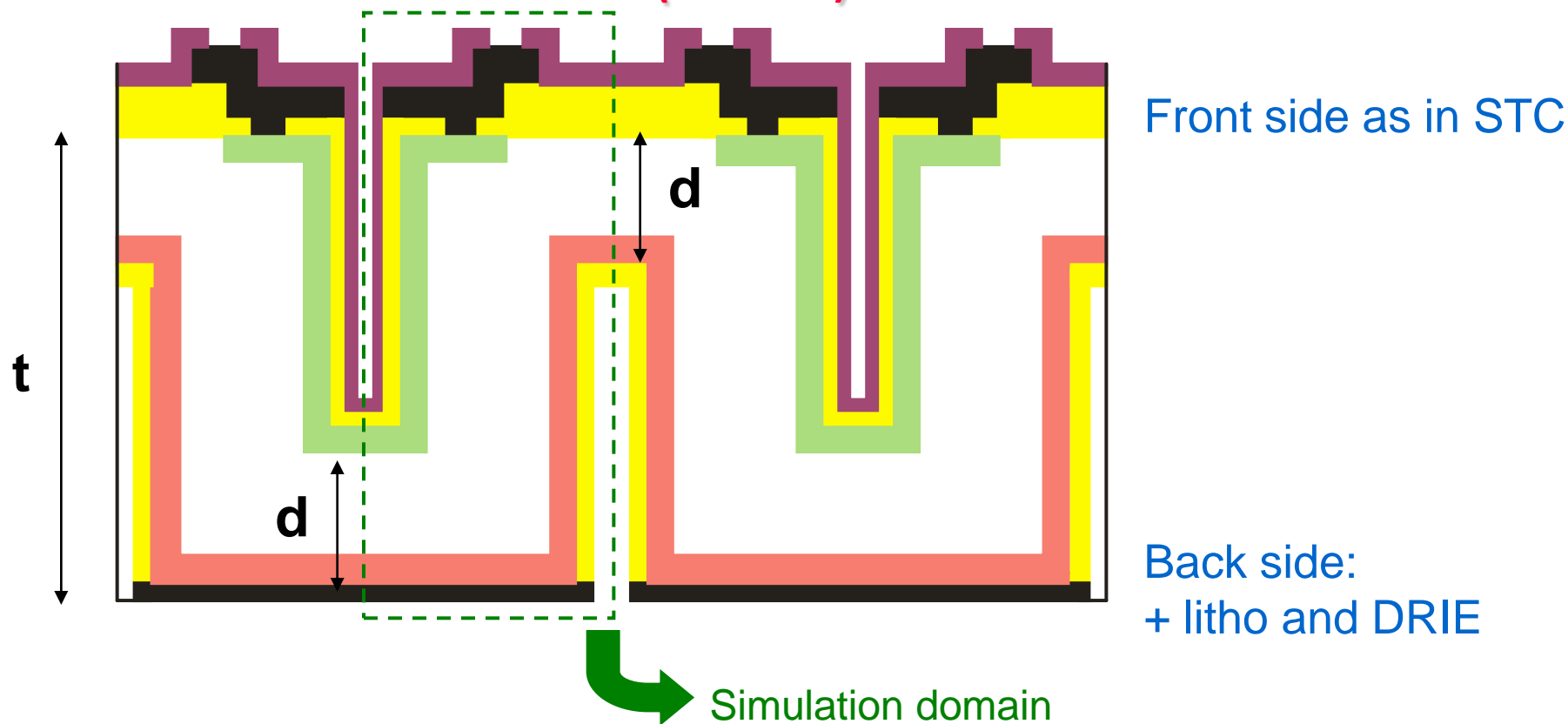
- 3D diodes and planar diodes (FZ, 500μm)
- Neutron irradiation at TRIGA reactor (6 fluences)
- Annealing 15 days at RT

Each column depletes half col. pitch

→ the lateral depletion voltage is very low.



3D Double-side Double-Type Column (DDTC) detectors

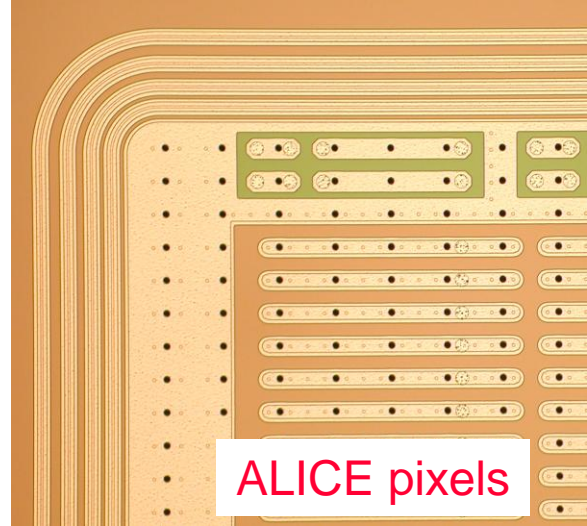
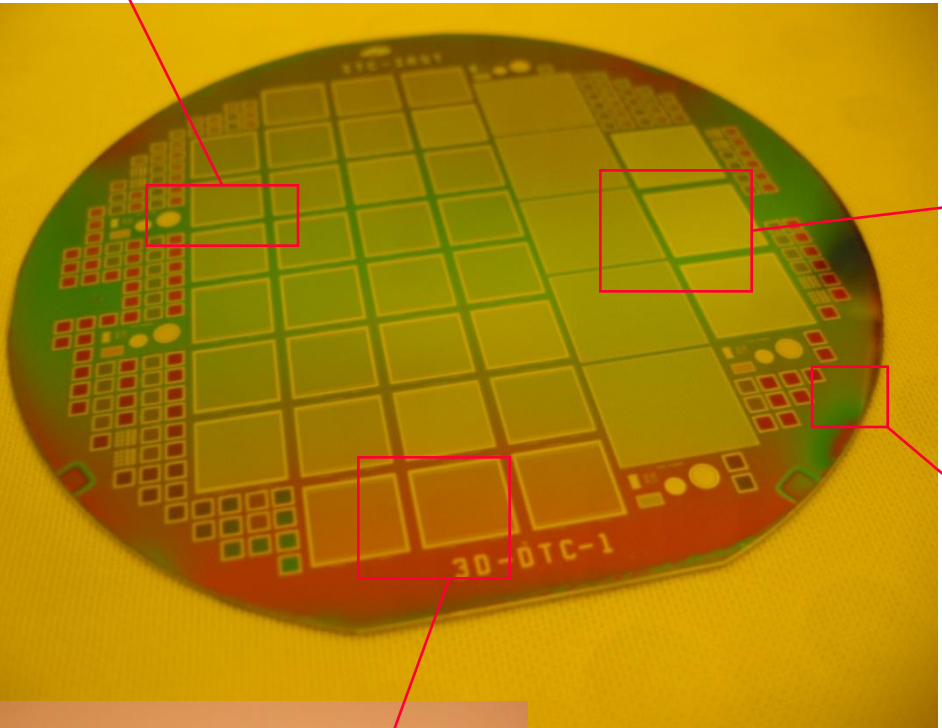


- Detector concept able to ease the fabrication process
- Expected to have performance comparable to standard 3D detectors

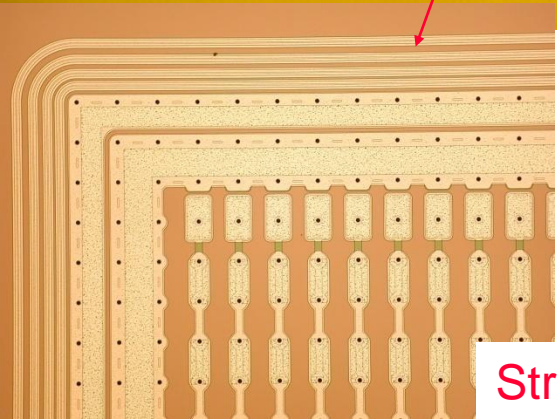
(if d is much smaller than t)

3D-DTC-1: some pictures

Planar TS



ALICE pixels



Strip detectors

3D diodes:
16x16 or 20x20
column array



DTC 80

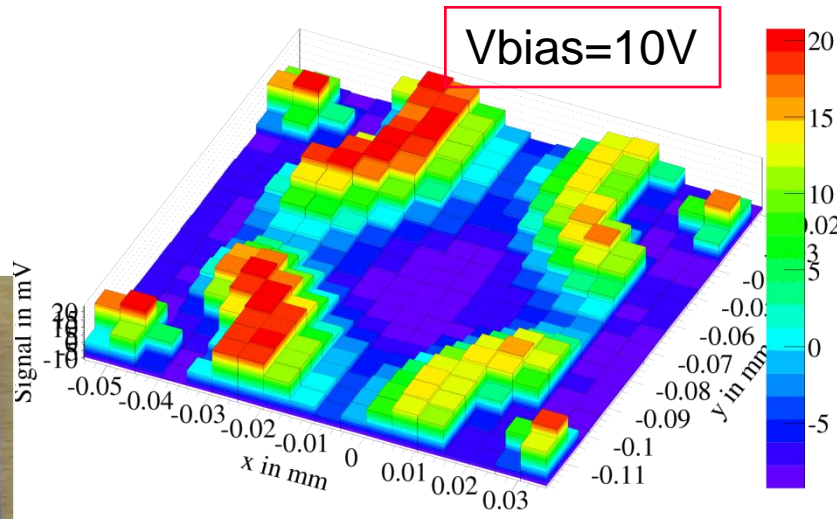
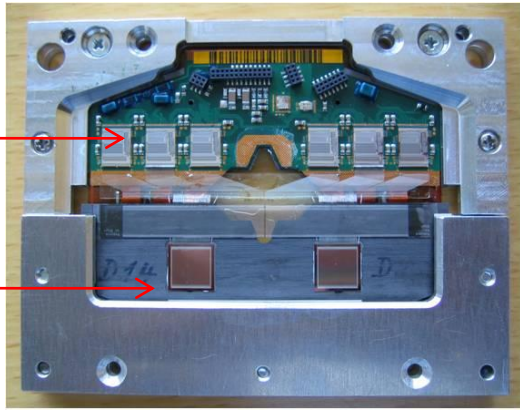
Position resolved CCE with ATLAS SCT readout

(Univ. Freiburg)

DEVICES: long strip detectors

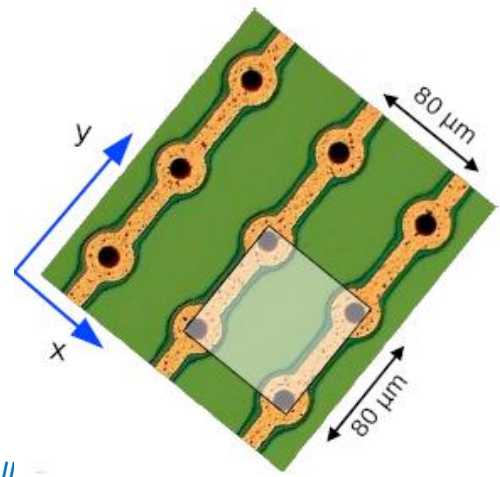
ABCD3T binary chip
20ns shaping time

Detectors



SETUP:

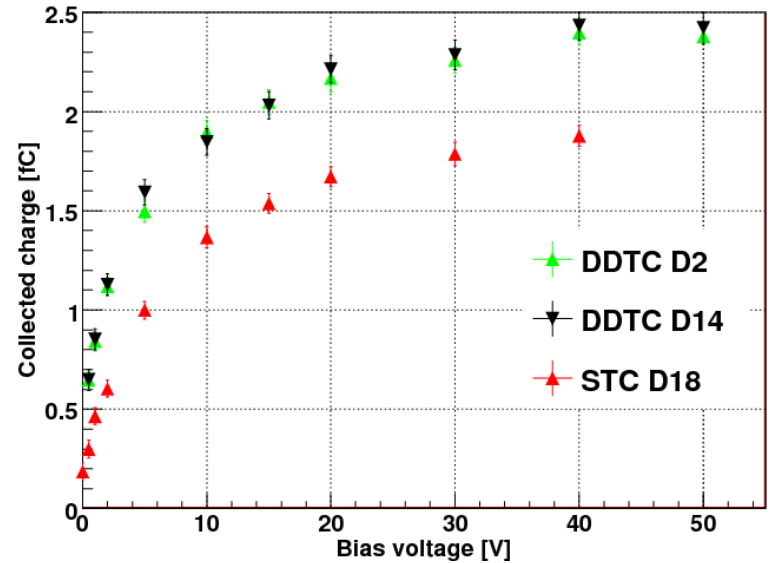
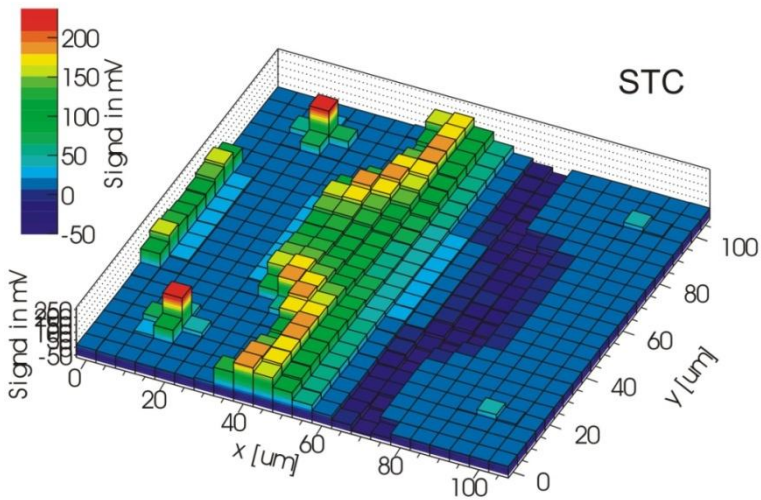
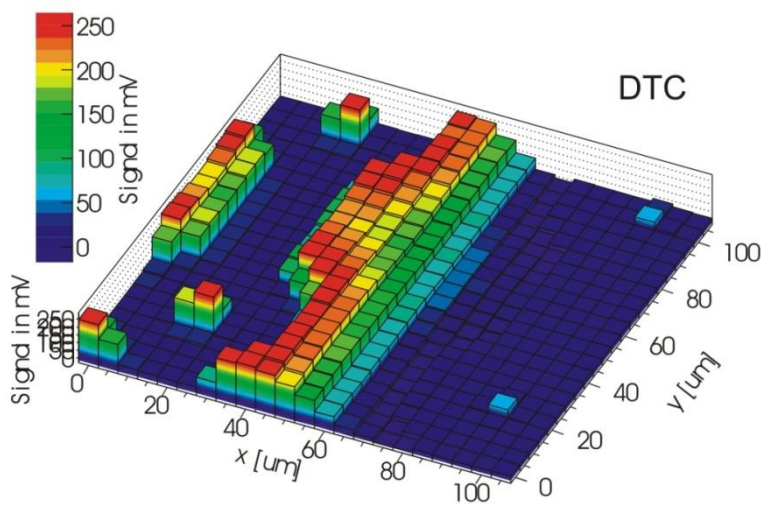
- 982 nm IR laser – light spot diameter 4-5 μm
- Pulse width \sim 1-2ns, synchronized with DAQ
- ATLAS SCT binary readout, shaping time 20 ns



DTC vs STC

Setup:

- Sr⁹⁰ beta source, MIP like charge deposition within the active area
- Events triggered by two scintillators in coincidence



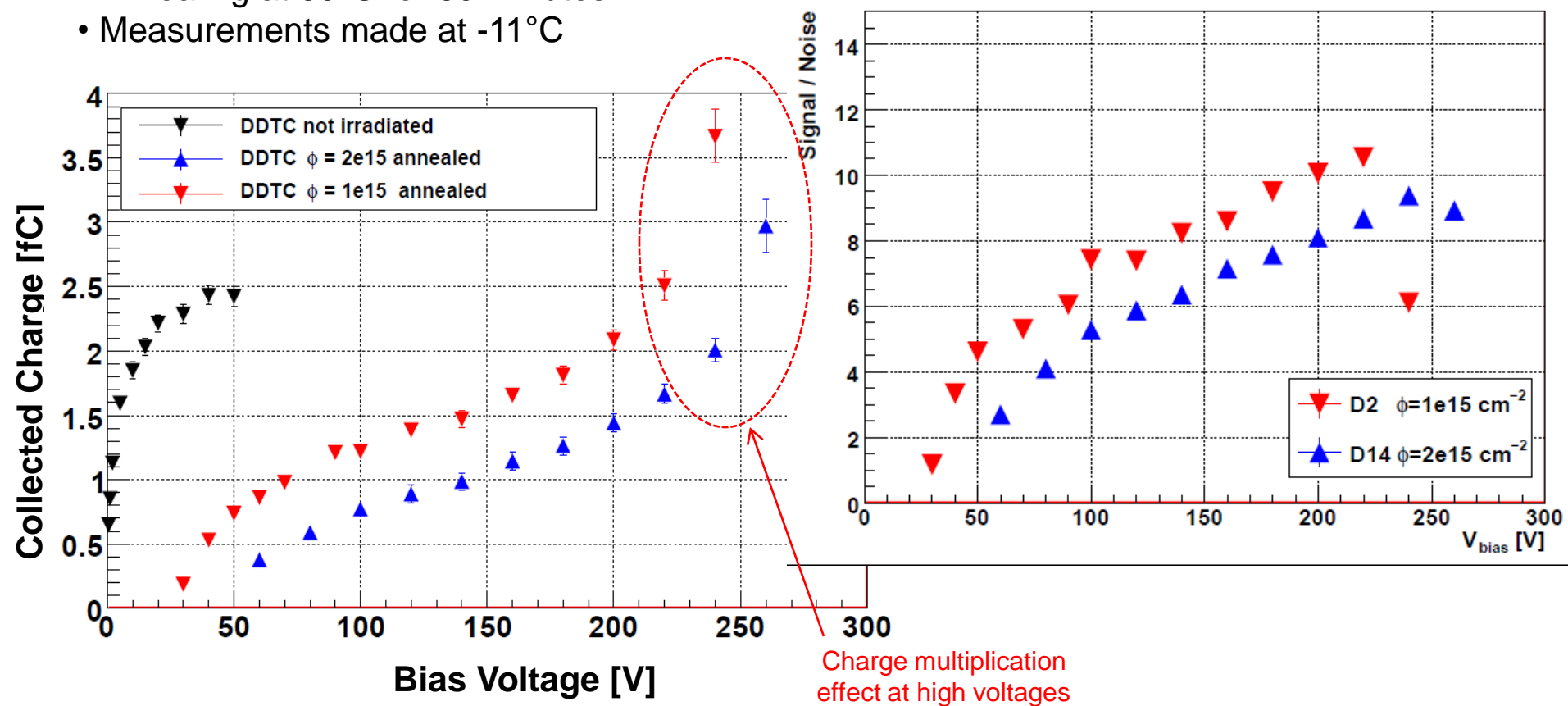
	Max	Negative
DDTC	250mV	-5mV
STC	180mV	-50mV

In agreement with
laser measurements:
**DDTC collects more charge
than STC**

Beta source tests after irradiation

^{90}Sr β source setup

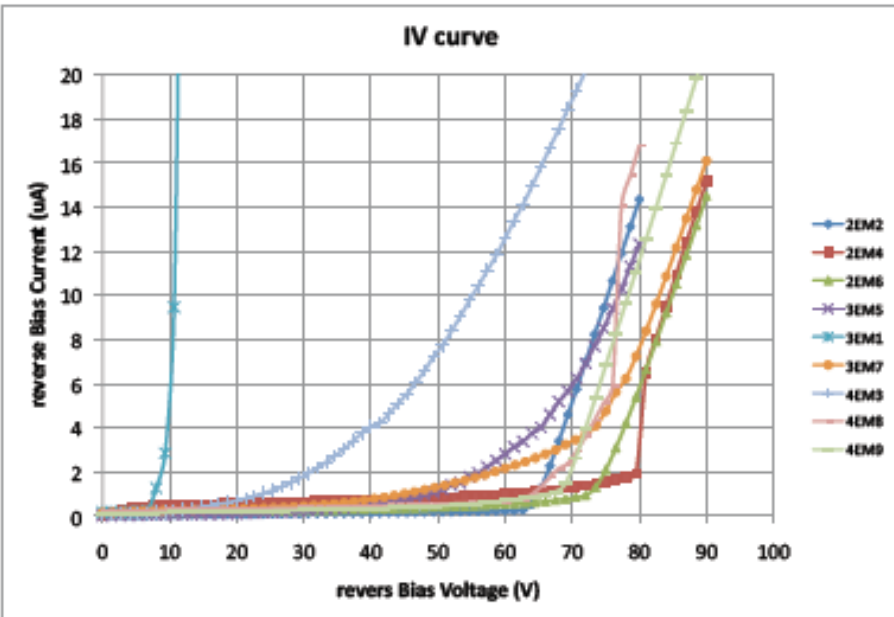
- Strip detectors read-out with ABCD3T binary chip, 20ns shaping time
- After irradiation with 24 MeV protons up to a fluence of $2 \times 10^{15} \text{ cm}^{-2}$
- Annealing at 60°C for 80 minutes
- Measurements made at -11°C



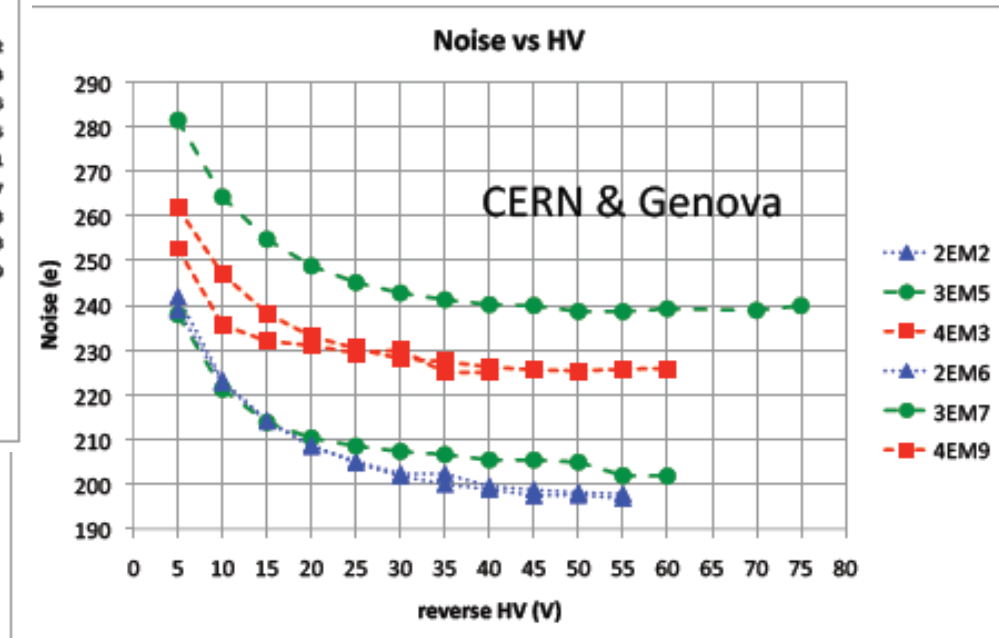
Initial results with ATLAS pixels

ATLAS pixel detectors with different column configurations assembled with FE-I3 ATLAS ROC (bump bonding at SELEX SI)

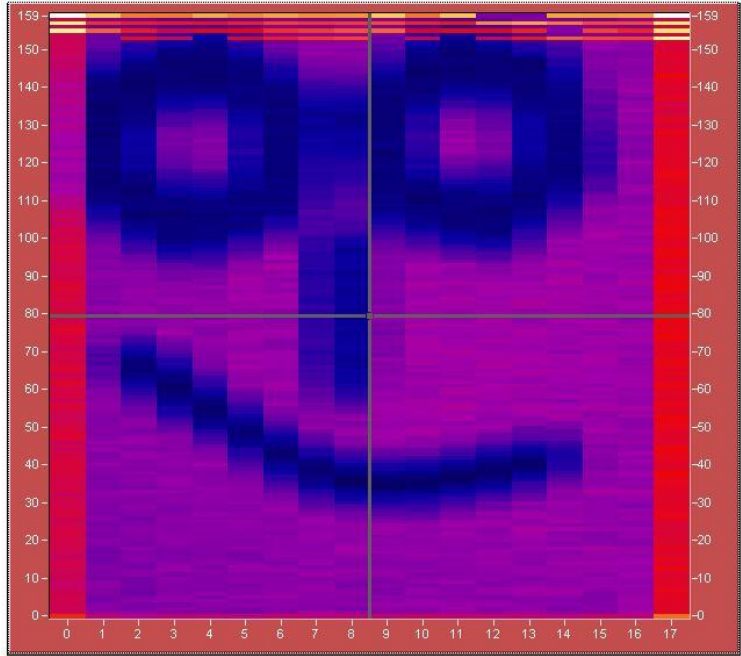
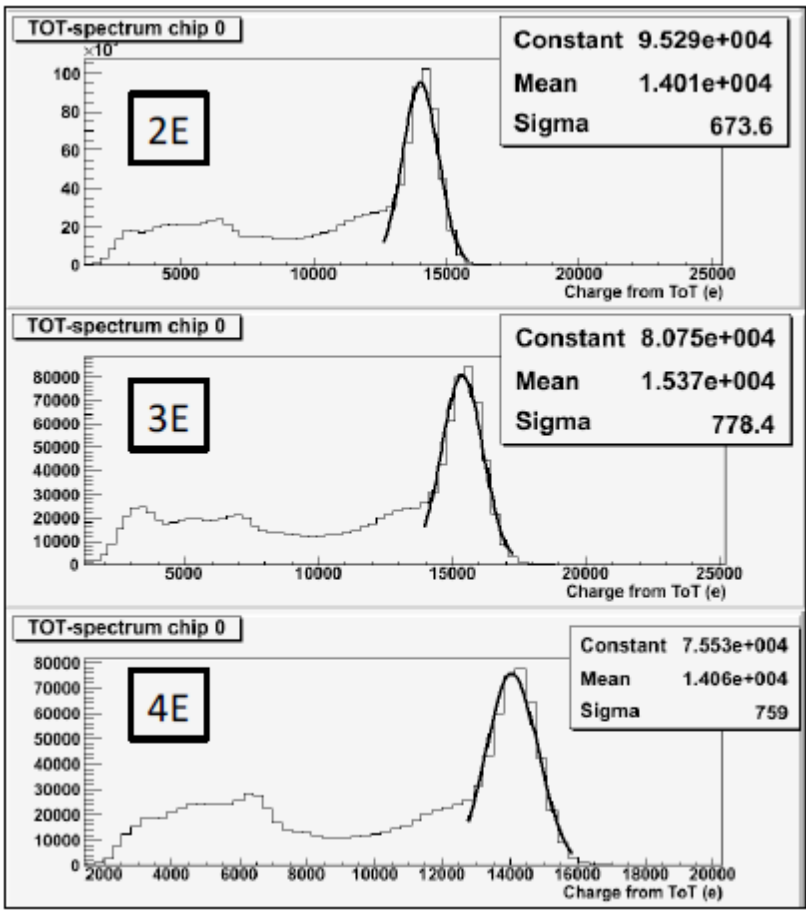
Leakage current



Noise scan



²⁴¹Am source preliminary tests



SINGLE FE **MODULE**

PLOT MODE
 RAW HITS

FE INDEX: 0

TOT FOR THIS Q: 25000

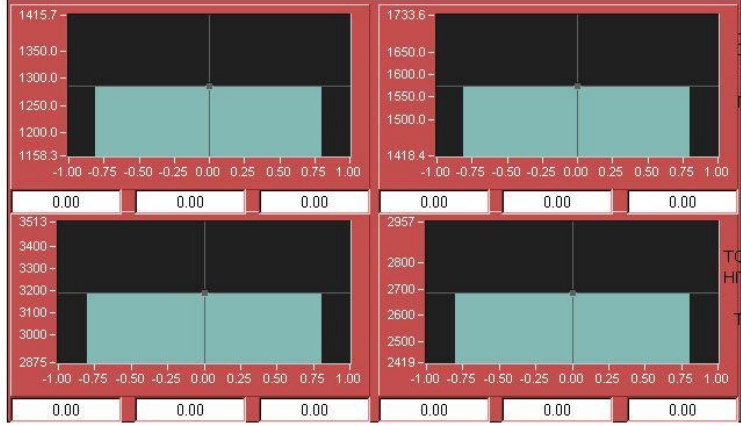
CHIP LABELS
 CHIP LABELS OFF

COLOUR MODE **SCALING MODE**
 COLOUR SPECTRUM 2-COL INTERPOLATION
 AUTOMATIC SCALING USER CONTROLLED

XWIRES: 9 80 1287 0.0 1287.0

HITMAP FLOOR
 256 055 055 055
 FLOOR AT 0

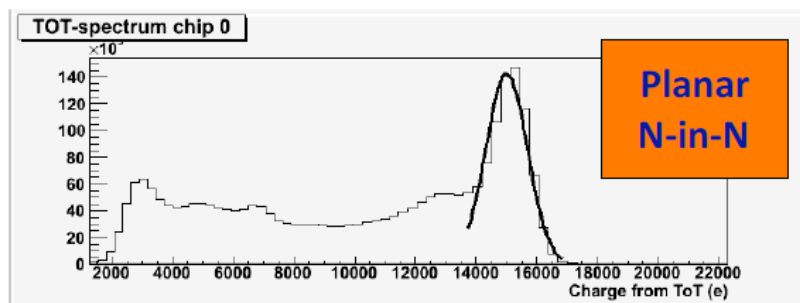
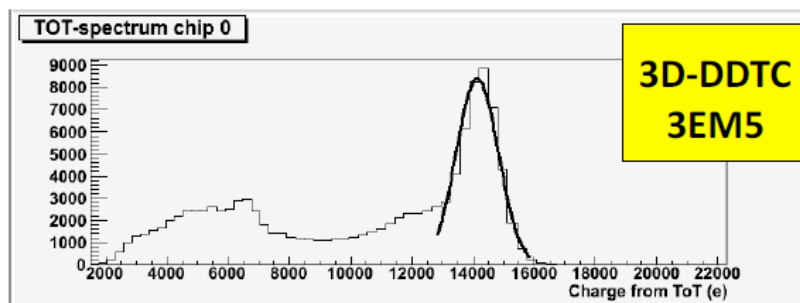
HITMAP CEILING
 256 055 055 055
 CEILING AT 4332



Source test (Am-241)

Preliminary measurement with **Am-241** source in comparison with **ATLAS N-in-N Planar sensor single-module**

Spectrum as a sum over all pixel without any clustering



Detector	Peak (10^4 e)	Sigma (e)
3D-2EM2	1.411	695.3
3D-2EM6	1.401	673.6
3D-3EM5	1.414	686.2
3D-3EM7	1.537	778.4
3D-4EM3	1.406	759.0
3D-4EM8	1.383	775.2
3D-4EM9	1.415	760.0
Planar (N-in-N)	1.501	688.4

See the expected 60keV peak

Attività in corso

Appena terminato un secondo lotto 3D-DDTC2: n-on-p, 200- μm , doppie colonne non passanti (160 μm giunzione 180 μm ohmiche)

In fabbricazione

3D-DDTC3: n-on-p, 250- μm thick substrate, full 3D detectors (passing-through) columns.

Per maggiori informazioni

<http://tredi.fbk.eu/>